NASA/TM—2012-217605

Variable-Speed Power-Turbine Research at Glenn Research Center

Gerard E. Welch, Ashlie B. McVetta, Mark A. Stevens, and Samuel A. Howard
Glenn Research Center, Cleveland, Ohio

Paul W. Giel
ASRC Aerospace Corporation, Cleveland, Ohio

Ali A. Ameri
The Ohio State University, Columbus, Ohio

Waiming To
University of Toledo, Toledo, Ohio

Gary J. Skoch and Douglas R. Thurman
U. S. Army Research Laboratory, Glenn Research Center, Cleveland, Ohio

July 2012

NASA STI Program . . . in Profile

Since its founding, NASA has been dedicated to the advancement of aeronautics and space science. The NASA Scientific and Technical Information (STI) program plays a key part in helping NASA maintain this important role.

The NASA STI Program operates under the auspices of the Agency Chief Information Officer. It collects, organizes, provides for archiving, and disseminates NASA's STI. The NASA STI program provides access to the NASA Aeronautics and Space Database and its public interface, the NASA Technical Reports Server, thus providing one of the largest collections of aeronautical and space science STI in the world. Results are published in both non-NASA channels and by NASA in the NASA STI Report Series, which includes the following report types:

- TECHNICAL PUBLICATION. Reports of completed research or a major significant phase of research that present the results of NASA programs and include extensive data or theoretical analysis. Includes compilations of significant scientific and technical data and information deemed to be of continuing reference value. NASA counterpart of peer-reviewed formal professional papers but has less stringent limitations on manuscript length and extent of graphic presentations.

- TECHNICAL MEMORANDUM. Scientific and technical findings that are preliminary or of specialized interest, e.g., quick release reports, working papers, and bibliographies that contain minimal annotation. Does not contain extensive analysis.

- CONTRACTOR REPORT. Scientific and technical findings by NASA-sponsored contractors and grantees.

- CONFERENCE PUBLICATION. Collected papers from scientific and technical conferences, symposia, seminars, or other meetings sponsored or cosponsored by NASA.

- SPECIAL PUBLICATION. Scientific, technical, or historical information from NASA programs, projects, and missions, often concerned with subjects having substantial public interest.

- TECHNICAL TRANSLATION. English-language translations of foreign scientific and technical material pertinent to NASA's mission.

Specialized services also include creating custom thesauri, building customized databases, organizing and publishing research results.

For more information about the NASA STI program, see the following:

- Access the NASA STI program home page at *http://www.sti.nasa.gov*

- E-mail your question to *help@sti.nasa.gov*

- Fax your question to the NASA STI Information Desk at 443–757–5803

- Phone the NASA STI Information Desk at 443–757–5802

- Write to:
  STI Information Desk
  NASA Center for AeroSpace Information
  7115 Standard Drive
  Hanover, MD 21076–1320

Variable-Speed Power-Turbine Research at Glenn Research Center

Gerard E. Welch, Ashlie B. McVetta, Mark A. Stevens, and Samuel A. Howard
Glenn Research Center, Cleveland, Ohio

Paul W. Giel
ASRC Aerospace Corporation, Cleveland, Ohio

Ali A. Ameri
The Ohio State University, Columbus, Ohio

Waiming To
University of Toledo, Toledo, Ohio

Gary J. Skoch and Douglas R. Thurman
U. S. Army Research Laboratory, Glenn Research Center, Cleveland, Ohio

National Aeronautics and
Space Administration

Glenn Research Center
Cleveland, Ohio 44135

July 2012

Acknowledgments

Variable-Speed Power-Turbine Research at Glenn Research Center

Gerard E. Welch, Ashlie B. McVetta, Mark A. Stevens, and Samuel A. Howard
National Aeronautics and Space Administration
Glenn Research Center
Cleveland, Ohio 44135

Paul W. Giel
ASRC Aerospace Corporation
Cleveland, Ohio 44135

Ali A. Ameri
The Ohio State University
Columbus, Ohio 43210

Waiming To
University of Toledo
Toledo, Ohio 43606

Gary J. Skoch and Douglas R. Thurman
U.S. Army Research Laboratory
Glenn Research Center
Cleveland, Ohio 44135

Abstract

The main rotors of the NASA Large Civil Tilt-Rotor (LCTR) notional vehicle operate over a wide speed-range, from 100 percent at takeoff to 54 percent at cruise. The variable-speed power turbine (VSPT) offers one approach by which to effect this speed variation. VSPT aerodynamics challenges include high work factors at cruise, wide (40° to 60°) incidence-angle variations in blade and vane rows over the speed range, and operation at low Reynolds numbers. Rotordynamics challenges include potential responsiveness to shaft modes within the 50 percent VSPT speed-range. A research effort underway at NASA Glenn Research Center, intended to address these key aerodynamic and rotordynamic challenges, is described. Conceptual design and 3-D multi-stage RANS and URANS analyses, conducted internally and under contract, provide expected VSPT sizing, stage-count, performance and operability information, and maps for system studies. Initial steps toward experimental testing of incidence-tolerant blading in a transonic linear cascade are described, and progress toward development/improvement of a simulation capability for multistage turbines with low Reynolds number transitional flow is summarized. Preliminary rotordynamics analyses indicate that viable concept engines with 50 percent VSPT shaft-speed range. Assessments of potential paths toward VSPT component-level testing are summarized.

Nomenclature

AN^2	product of annulus area and shaft-speed squared
C_p	$\frac{p_{0,1}-p}{\frac{1}{2}\rho U^2}$, local pressure coefficient
C_{ptot}	$\frac{p_{0,1}-p_0}{p_{0,1}-p_2}$, local total-pressure coefficient
c_x	axial chord
h_0	total specific enthalpy
i, i_{des}	incidence, design incidence
k	turbulent kinetic energy
k_1	laminar kinetic energy
N	power-turbine shaft speed
N^*	$N/N_{100\%}$, fraction of 100 percent speed
Nu	Nusselt number
PR_{TT}	overall total-pressure ratio
p_0, p	total and static pressure
Re_{cx}	Reynolds number based on axial chord
s	blade pitch, or specific entropy
T_0	total temperature
TR_{TT}	overall total-temperature ratio
Tu	turbulence intensity
$\underline{u}$	(u_x, u_θ, u_r), absolute velocity
U	blade speed at pitchline
X_{pk-pk}	vibration amplitude, peak-to-peak
Z	$\frac{s}{c_x}\frac{\rho u_x(u_{\theta,1}-u_{\theta,2})}{p_{0,r,1}-p_2}$, Zweifel loading parameter
α, β	absolute and relative flow angles
η_{TT}	adiabatic efficiency (total-to-total)
ρ	density
ψ	$\Delta h_0/U^2$, work factor
ϕ	u_x/U, flow coefficient
$\overline{\omega}$	$\frac{\bar{p}_{0,1}-\bar{p}_{0,2}}{\bar{p}_{0,1}-\bar{p}_2}$, loss coefficient (area-averaged)
ω	specific dissipation rate of turbulence

Introduction

The vertical takeoff and landing (VTOL) and Mach 0.5 cruise capability of the NASA Large Civil Tilt-Rotor (LCTR, (Refs. 1 and 2) Figure 1) is envisaged to increase throughput in the national airspace (Refs. 1 and 3). A key challenge of the LCTR is the variation in main-rotor tip-speed from 650 ft/s (100 percent N^*) at sea-level VTOL to 350 ft/s (54 percent N^*) at 28 k-ft cruise as required to minimize mission fuel-burn. The variable-speed power-turbine (VSPT), driving the rotor through a fixed gear-ratio transmission, provides one approach for effecting this wide speed variation. The VSPT approach is used in the V-22 where the output speed of the AE1107 engine varies speed in the range 80 percent $< N^* \leq 100$ percent (Ref. 3). The LCTR mission evidently widens the operational speed range of the main rotor, drive system, and VSPT power-shaft (54 percent $\leq N^* \leq 100$ percent) considerably.

Key Technical Challenges

The VSPT research effort at NASA Glenn Research Center (GRC) is intended to address key aerodynamic and mechanical (rotordynamic) challenges of the VSPT. The aerodynamic challenges include attainment of high turbine efficiency at high work factor, management of loss levels over a large (60°) incidence variation in all blade rows associated with the shaft-speed change, and operation at low Reynolds numbers with attendant sensitivity of transitional flow (Ref. 4). The loss levels in the transitional flow fields of low-pressure turbines (LPTs) operating at cruise altitudes (with Re < 100 k) are known to be impacted strongly by wake-induced unsteadiness (Ref. 5) as well. The mechanical challenges are associated with the required avoidance or management of responsive shaft, blade, and casing modes at critical speeds within the operational speed range of the VSPT shaft (Ref. 6).

While the VSPT approach to speed change is the subject of this paper, the main-rotor speed variation could alternatively be accomplished by using a two-speed (reduction gear-ratio) transmission (Ref. 7) (shifting) with a fixed-speed power turbine. The turbine of the two-speed transmission option shares the aerodynamic challenges associated with low-Re number operation and the need to avoid residence at shaft critical speeds during the shift maneuvers (Ref. 8). The distinguishing turbine benefits of the two-speed shifting option are associated with the ability to run the power turbine, throughout the mission, at the higher shaft speed of takeoff (100 percent N^*) with minimal incidence variation. Operation at the takeoff shaft-speed with design-intent air angles enables

Figure 1.—NASA Large Civil Tilt-Rotor notional vehicle (Ref. 1).

higher cruise and takeoff efficiency levels, achievable at lower design-point work factors, in lower weight, reduced stage-count turbine designs.

Research Approach

The VSPT technical challenges have motivated a research (Ref. 4) effort at GRC related to VSPT aerodynamics, rotordynamics, and component-level testing. These research activities were conducted internal to GRC and through contracted efforts with industry.

The aerodynamics research elements include:

i. VSPT requirements and conceptual design. Execute conceptual design of a VSPT to meet LCTR mission/engine requirements at the meanline level, to establish representative blade row performance levels and VSPT performance maps.

ii. Detailed design of incidence-tolerant blading. Conduct 3-D aero-design (computational) of incidence-tolerant rotor, vane, and EGV blade shapes using flow angles from the meanline analyses.

iii. Transonic cascade testing of 2-D sections. Test 2-D sections of the 3-D VSPT incidence-tolerant blading in GRC transonic linear cascade at LCTR-relevant Mach numbers, Reynolds numbers, incidence angle variations (>55°).

iv. Transition sub-model assessment/implementation. Develop a validated 3-D unsteady RANS simulation capability for unsteady low-Re transitional flows in multistage VSPT blade rows.

The rotordynamics research element addresses mechanical challenges associated with operation of a VSPT, with intent to identify potential constraints imposed on the aerodynamic design by mechanical issues associated with variable speed—for example, growth in shaft radius to meet torque capacity requirements and to manage responsiveness to shaft critical speeds (rotordynamics).

Finally, the component test element is to assess potential in-house and external test vehicles for component level VSPT experimentation.

Content

An overview of progress to-date on the research elements outlined above is provided herein. The paper includes sections related to VSPT conceptual aerodynamic design and analysis, experimental testing of incidence-tolerant blading, computational methods, rotordynamics, and an assessment of potential VSPT component test paths. A summary is provided at the conclusion of the paper.

VSPT Conceptual Aerodynamic Design and Analysis

The conceptual design and analysis of VSPTs for the LCTR mission was conducted by NASA and through NASA Research and Technologies for Aerospace Propulsion Systems (RTAPS) contracts with Williams Int., L.L.C. (Ref. 9) and Rolls-Royce North American Technologies (Refs. 10 and 11). The intent of the RTAPS efforts were to develop a conceptual design of the VSPT for the LCTR application to a level required to emerge the key technical challenges—both aerodynamic and rotordynamic—to identify research required to overcome these challenges, and to define a path forward, and the test-plan, for a VSPT component-level test.

NASA, Williams International (WI) (Ref. 9) and Rolls-Royce North American Technologies (RR-NAT) (Ref. 10) arrived at a 4-stage VSPT design to meet the LCTR mission and engine cycle provided by the NASA engine performance group. Rolls-Royce carried out a second effort using a higher mass-flow-rate, growth AE1107C engine cycle, which led to a 3.5-stage configuration (Ref. 11). In all studies, the VSPT requirements were met without the use of variable geometry.

The turbine requirements of the VSPT concept design effort are provided below, followed by key findings from each conceptual design and aerodynamic analysis efforts by NASA and industry.

VSPT Requirements

The NASA LCTR notional vehicle (Figure 1) is envisaged to be a 90 passenger aircraft with 100,000 lb_f takeoff gross weight. There are two engines per nacelle (and main rotor), currently conceived to be of the 7500 shp-class level. Two key LCTR mission points are 2 k-ft takeoff/hover and 28 k-ft, Mach 0.5 cruise. At takeoff, the main rotor and VSPT operate at 100 percent N^*, while at cruise the rotors and VSPT are slowed to 54 percent N^*. The LTRC engine requirements were established with the NASA engine performance group (Ref. 12). The corresponding VSPT requirements for the key takeoff and cruise operating points are provided in Table I.

TABLE I.—VSPT REQUIREMENTS AT KEY FLIGHT
POINTS OF LCTR MISSION (REF. 12)

Flight point	Takeoff	Cruise
Altitude	2k-ft	28 k-ft
VSPT shaft-speed ($N/N_{100\%}$)	100%	54%
Main-rotor tip-speed	650 ft/s	350 ft/s
Power, shp	4593	2328
Mass flow rate, lb_m/s	22.03	12.22
Specific power (Btu/lb_m)	147	135
Inlet temperature ($T_{0,4.5}$), R	2204	1812
Inlet pressure ($p_{0,4.5}$), psia	58.0	26.76
PR_{TT}	4.04	5.34
Corrected flow, lb_m/s	11.51	12.54
Corrected speed ($N_c/N_{c,100\%}$), %	102.3	60.8
Aft-stage unit-Re (in^{-1})*	70,000/in.	45,000/in.

*Based on static conditions at last stage rotor with exit relative Mach number of 0.7.

NASA Aerodynamic Design and Aero Analysis

VSPT Conceptual Design

The NASA conceptual aero-design approach for a 4-stage VPST of the LCTR application was outlined earlier (Refs. 4 and 13). The design air-angles were set at the cruise operating condition (54 percent N^*) where Reynolds numbers were lowest and work factors ($\Delta h_0/U^2$) were highest. Maximum vane and blade-row incidence levels were as high as negative 60° at takeoff (100 percent N^*). The turbine flow path, number of stages, and design air angles were determined using F. Huber's meanline design and off-design codes, which are constituents of the AFRL Turbine Design and Analysis System (TDAAS) (Ref. 14). The aerodynamic loading levels of the vanes (Zweifel coefficient) were set near unity so as to be consistent with operation with transitional flow (Ref. 15) and required incidence tolerance. The stage reaction levels were set near 0.45 and flow coefficients, u_x/U, at cruise were set near unity. The stage work splits were based on trades between optimum efficiency and management of maximum turning per stage. The rotors were tip-shrouded and leakage flows were neglected. Huber's off-design code (Ref. 14) (meanline) was used to assess off-design operation.

The design- (54 percent N^*, cruise) and off-design (100 percent N^*, takeoff) performance levels are spotted on the modified Smith Chart of Figure 2. AN^2 levels, 47.7×10^9 rpm^2·in^2 at 15,000 rpm takeoff speed, were based on strength-of-materials for anticipated turbine materials at the operating conditions of the LCTR VSPT. The average work factors from industry conceptual designs (Refs. 9, 10, and 16) are shown as well. The impact of adding a stage, from 3-stages to 4-stages, on efficiency corresponding to design work factor is evident. The gained VSPT efficiency at the higher stage count would be expected to come at the cost of increased weight to the VSPT. The sensitivity of the LCTR to the turbine weight and efficiency makes the stage count selection a deep trade that will aim to optimize the VSPT efficiency and weight, for optimal life, cost, and fuel burn.
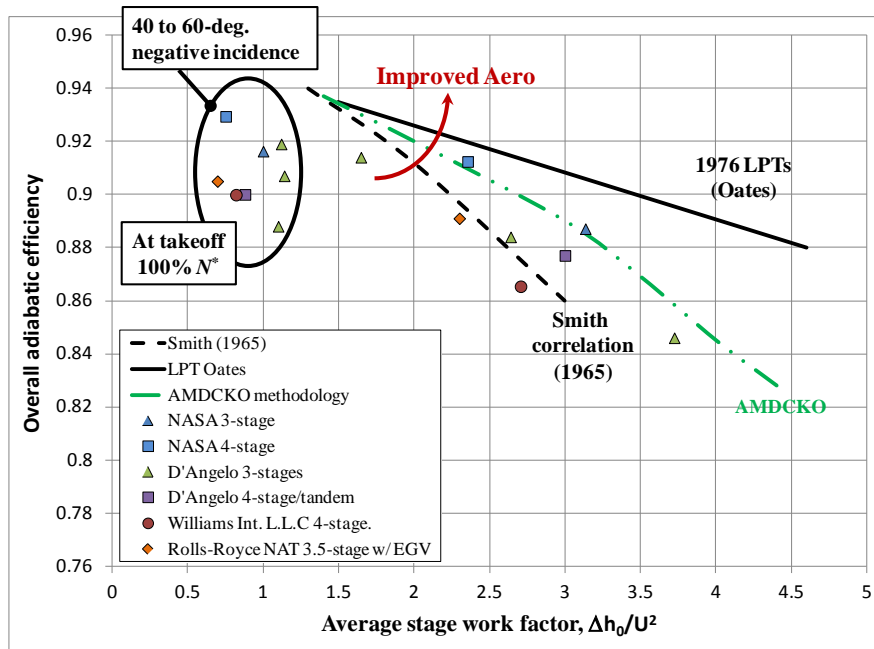
Figure 2.—Modified Smith chart showing meanline predicted design-point efficiency as a function of work factor for 3- and 4-stage VSPT meanline designs (Refs. 9, 10, 13, and 16) compared to Smith (Ref. 17) and Oates (Ref. 18) correlations and AMDCKO methodology (Refs. 19 to 21). Calculated performance levels at the off-design takeoff (100 percent N^*) are also shown.

The off-design efficiency level, corresponding to takeoff operation with strongly negative incidence (e.g., –60°) in all blade rows, is predicted (Figure 2) by meanline analyses (Refs. 4, 9, 10, 13, and 16) to be higher than that at design-point where work factor is highest (Refs. 4 and 13). The overall loss levels are lower at the reduced work factors and aerodynamic loading levels, Z, of takeoff. The profile loss component—associated with boundary-layer and shocks—at negative incidence is near that of the higher loaded design air angles (see Ref. 4) whereas the secondary-flows and leakage flows (3-D) predicted at the lower aerodynamic loading levels of off-design are substantially lower than at the on-design cruise condition. The impact of this counterintuitive efficiency increase as the turbine unloads biases the selected VSPT design speed toward the cruise speed (54 percent N^*).

3-D Blading Design

The predicted loss levels at off-design are strongly dependent on the loss correlations in the meanline tool used (Refs. 9, 10, and 13). Therefore a 3-D CFD study of a representative embedded 1.5-stage (Rotor 1, Stator 2, and Rotor 2, Figure 3) of the 4-stage NASA VSPT was conducted to verify the efficiency versus speed trend of the meanline code held when 3-D flow structures (see Figure 3 and Figure 4) were present. The 3-D aero-design of the blading for the 1.5-stage (R1/S2/R2) of the present study was described in detail earlier (Ref. 13). R1 and R2 were shrouded, and leakage flows were neglected. With
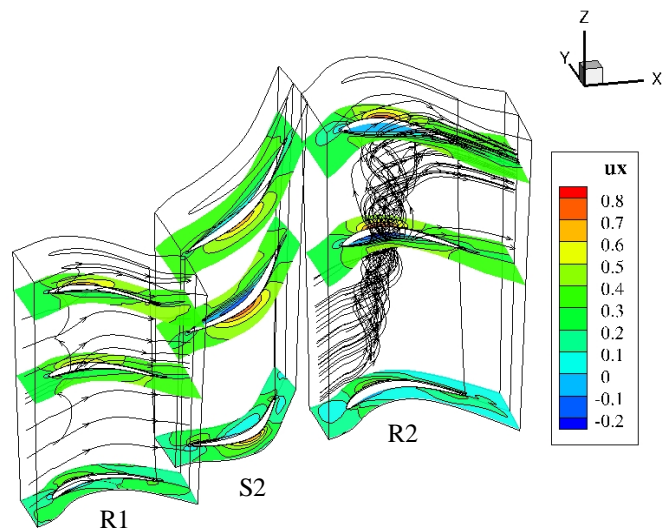

Figure 3.—Computed contours of axial velocity and stream-lines in R1 and R2 at the 100% N^* off-design take-off point (reproduced from Ref. 22).

design air angles from the meanline design code, the AFRL Turbine Design and Analysis System (TDAAS (Ref. 14)) was used to design, optimize, and stack 2-D airfoil sections, at hub, midspan, and tip, into a 3-D blade geometry. The chordwise-location of maximum loading was influenced by the findings of Gier et al. (Ref. 15) concerning efficiency, Re-lapse, and sensitivity to incidence in low pressure turbines designed for
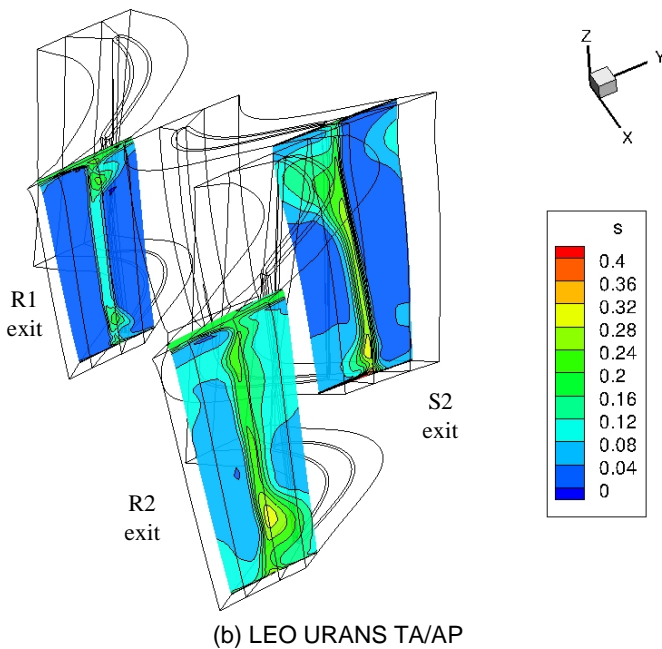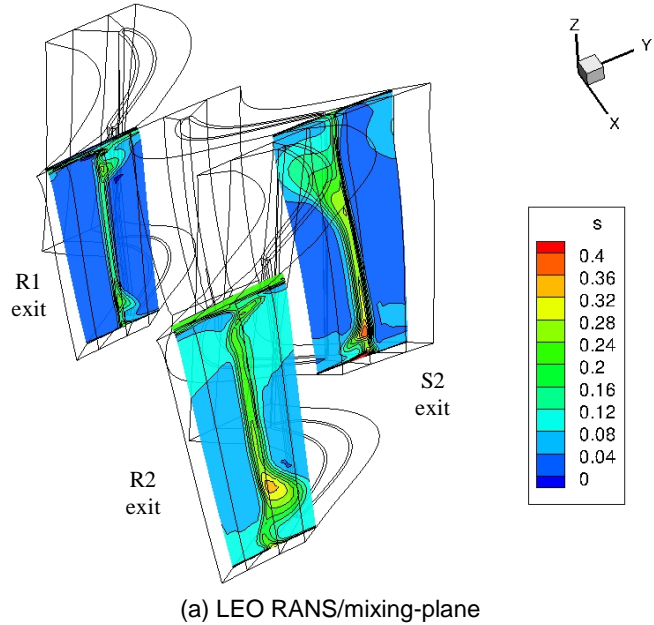
(a) LEO RANS/mixing-plane

(b) LEO URANS TA/AP

Figure 4.—Computed contours of entropy at the blade-row exit planes from (a) LEO RANS/mixing-plane and (b) time-averaged, average-passage (TA/AP) URANS calculations at design point (54 percent N^*, 28 k-ft cruise).

low-Re operation. The 2-D sections (provided in Ref. 13) were stacked on their center of gravity along a radial stacking axis. No dihedral was considered, though the benefits of 3-D aerodynamic design, in managing the secondary flow fields, is well documented (Ref. 5).

Efficiency/Speed Trend Verification

Using the embedded 1.5-stage geometry, 3-D RANS/mixing-plane computations were conducted using the NASA SWIFT (Ref. 22) code at the cruise (54 percent N^*, 28 k-ft) and takeoff (100 percent N^*, 2 k-ft) conditions. The meanline and 3-D simulations were found to agree in terms of the variation of efficiency with VSPT operating speed. Consistent with meanline analyses, the blade-row loss levels were generally found to be lower at the off-design conditions where, though operating with 40° to 60° of negative incidence, the blade rows are unloaded. An exception to this general trend of higher efficiency at off-design was found in Rotor 2, attributable to the impact of the 3-D pressure-side cove vortex. This finding may push future rotor airfoil designs toward thicker sections that admit less of a cove separation. Enhancement of the meanline secondary loss model for rotors at extreme negative incidence, to account for increased loss due to such 3-D structures, may be warranted as well.

The agreement between 3-D RANS computations and the meanline both corroborated the incidence correlation of the meanline code—with the exception of R2 deficiency noted above—and supported the conceptual design approach that established the design speed at the lowest operating shaft speed (54 percent N^*, cruise). In practice, the specific VSPT design speed is expected to be strongly biased toward the cruise shaft-speed, and selected so as to minimize mission fuel burn.

Impact of Unsteadiness—URANS Simulations

The RANS/mixing-plane analysis (Ref. 13) was extended to 3-D unsteady RANS (URANS) in an effort to assess the influence of unsteadiness associated with blade-row interaction on the design- and off-design aerodynamic performance of a VSPT for the NASA LCTR (Ref. 23). The extension was motivated by the potential impact on VSPT performance of flow physics not accounted for in mixing-plane analyses: additional entropy production associated with the unsteady forcing of the vortical structures (e.g., the pressure-side cove R2 of Figure 3); spatiotemporally resolved loss production associated with wake transport and stretching (Ref. 24); transport of streamwise vorticity to/from blade rows and associated impact of vorticity associated with secondary flow field of one blade row on the instantaneous and time-mean flow fields of downstream blade rows (Ref. 25); and, the deterministic vortical forcing of transitional boundary-layers by wakes from upstream blade rows (Refs. 26 and 27). The computations of the RANS/mixing-plane study (Ref. 13) were repeated using the commercially available WAND and LEO grid and flow solvers (Ref. 28) in both RANS/mixing-plane and sector-periodic URANS mode. Results from the RANS/mixing-plane and time-averaged, average-passage (TA/AP) URANS results are provided in Figure 4 where the blade row exit contours of the solutions are compared at the cruise conditions.

The agreement between the time-averaged/URANS and the RANS/mixing-plane solutions was excellent. The unsteadiness due to blade-row interaction was found to degrade work and efficiency levels in Rotor 2, which was most impacted by the upstream blade rows of the embedded R1/S2/R2 1.5-stage simulation. Quantification of the efficiency degradation (approximately 1 point) associated with unsteadiness, vis-à-vis comparison of efficiency predicted using the RANS/mixing-plane and sector-periodic URANS computations, was unfortunately rendered inconclusive by a mixing-plane issue encountered (see Ref. 23). The trend of efficiency with changing VSPT shaft speed from the URANS simulation, from 54 percent N^* (28 k-ft, cruise) to 100 percent N^* (2 k-ft, takeoff), agreed with the corresponding trends from the two RANS/mixing-plane codes (SWIFT and LEO) and the meanline codes (Ref. 14) used for turbine design.

Williams International Aerodynamic Design and Analysis (Ref. 9)

VSPT Conceptual Design

In the Williams International (WI) RTAPS effort (Ref. 9), the shaft-speed at which to design the VSPT was determined through a sensitivity study of mission fuel burn versus the design speed. Turbine efficiencies were calculated using a meanline tool proprietary to WI with loss correlations rooted in the open literature (consistent with AMDCKO (Refs. 19 to 21). The results are reproduced in Figure 5 where it was found that the minimum fuel burn was achieved when the design point was set at approximately 70 percent N^* (as opposed to the 54 percent N^* argued in the NASA work above). The trade between high and low flow coefficient ($\phi = u_x / U$) turbine designs—i.e., low/high turning versus high/low Mach numbers (Figure 5)—high and low work factor, $\Delta h_0/U^2$, designs, and number of stages was also investigated. The conclusions were as follows (Ref. 9): i.) there was no compelling evidence found at the meanline level to support a preferred selection of flow coefficient (Figure 5); ii.) of 3- and 4-stage designs, all 15000 rpm at 100 percent N^*, a high work-factor (lower radius) 4-stage design was optimal in terms of mission fuel burn.

3-D Blading Design

A 3-D aero design was executed for the eight blade rows of the 4-stage VSPT, based on a meanline design at a 75 percent N^* (Ref. 9). Three 2-D sections were stacked for each of the eight blade rows. The 3-D sections were created using a WI interactive design tool for blade geometry, structural analysis, 2-D aero, and 3-D stacking. Design iterations were analyzed in a 3-D multistage Euler/RANS/mixing-plane solver (VORTEX) in Euler mode, and final designs were assessed using 3-D RANS/mixing-plane with $k-\omega$ turbulence modeling in VORTEX.
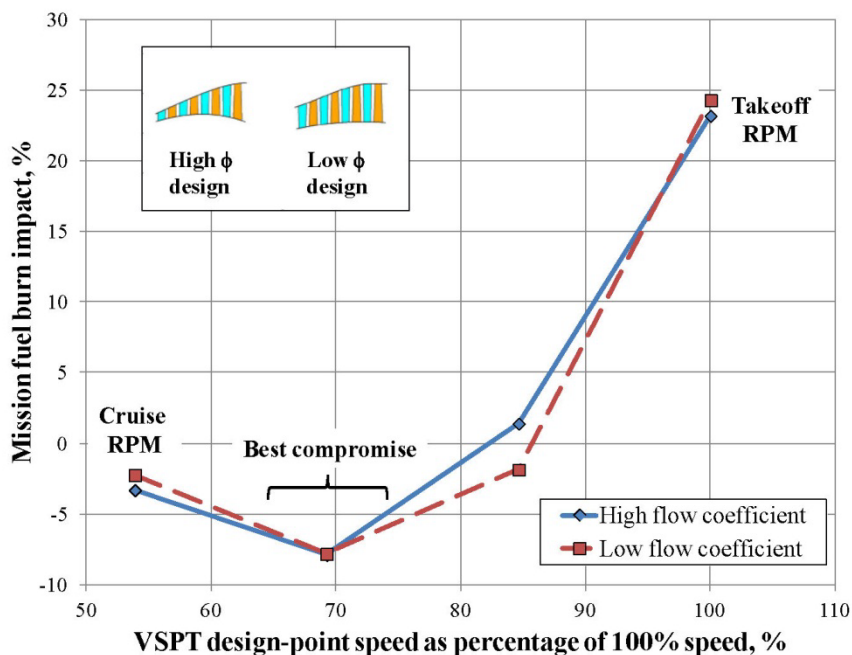

Figure 5.—Mission fuel burn as a function of VSPT design speed, showing insets for turbine designs at low and high flow coefficient (Ref. 9).

The embedded third stage vane (S3) and blade (R3) blade were analyzed using the steady VORTEX flow solver to assess the impact of turbulence sub-model selection and blade thickness distributions. The shaft speed, N^*, was varied at a fixed stage pressure ratio. Regarding blade thickness, the intuition is that larger radius leading edges (and resultant blade thicknesses) afford incidence-tolerance, which must the traded against higher loss levels associated with higher through-flow Mach numbers. The study examined whether a thin blade (lower Mach numbers) might improve turbine efficiency over a traditional WI blade design, or whether admittance of a pressure-side cove separations at off-design, and subsequent centrifuging in thinned rotor blades (cf. NASA Rotor 2 of Figure 3), would outweigh gains. The thinner blades were not found to offer overall benefit over traditional blade thickness (area) schedules (Ref. 9).

Assessment of Performance/Speed Trend

A key finding of the WI study is reproduced in Figure 6, where efficiency of a 1.5-stage (R2/S2/R3) embedded stage, computed using the 3-D RANS/mixing plane VORTEX solver is provided. The inlet conditions and pressure ratio of the embedded 1.5-stage of WI were held constant as speed was changed. The computed efficiency versus speed trend of the WI meanline tool and the 3-D computations are in qualitative agreement except that the roll-off in efficiency at negative incidence is more severe in the meanline than in the CFD. The

efficiency at cruise is again found (see Fig. 2) to be lower than that at takeoff (extreme off-design). This finding corroborates the embedded 1.5-stage results reported by NASA (Ref. 13 and 23), which are also plotted on Figure 6 The CFD results support the argument that the WI design-point speed (here 75 percent of takeoff speed) might optimally be further reduced, giving stronger bias to cruise operation.

Rolls-Royce North American Technologies Aerodynamic Design and Analysis

RR-NAT was awarded two NASA RTAPS contracts for an incidence-tolerant blade design effort (Ref. 10) and a VSPT study effort (Ref. 11) which paralleled the WI effort described above.

VSPT Conceptual Design

In the blade design contract (Ref. 10), meanline analyses were used to determine that a 4-stage turbine was preferred to meet the LCTR engine requirements for the NASA mission provided. The meanline analysis was influenced by lessons learned from RR-NAT work done under subcontract to Boeing in a separate NASA contract (Ref. 29) and an early NASA concept design (Ref. 4). The VSPT was tailored to maintain matched stage flow coefficients near unity, effectively keeping axial Mach numbers below 0.5 through the four stages and balancing the stage work factors.
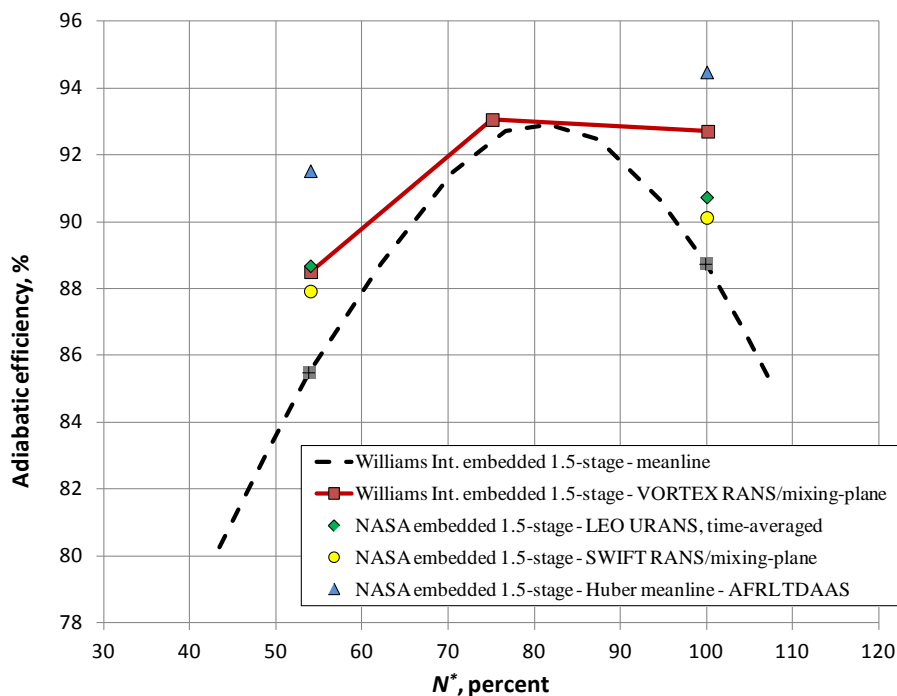

Figure 6.—Variation of computed efficiency with speed for Williams Int. embedded 1.5-stage and NASA embedded 1.5-stage of 4-stage VSPTs for the LCTR mission.
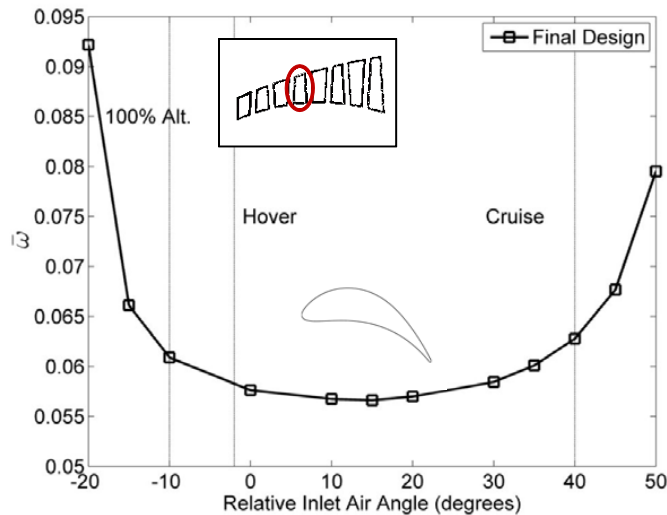
Figure 7.—Computed midspan loss as a function of inlet relative air angle for Rotor 2 of 4-stage VSPT for LCTR application (Ref. 11), showing VSPT incidence-tolerant blade as inset.

Incidence-Tolerant Blade Design (Ref. 10)

The second rotor (R2) of the RR-NAT 4-stage was selected as a representative embedded bladerow, both in terms of design turning and incidence range requirements between cruise and takeoff, for a 3-D blade design. Through-flow analysis was conducted using an RR-NAT axisymmetric streamline-curvature/radial-equilibrium solver. The 2-D streamline solution provided boundary conditions for subsequent 3-D design of R2.

An incidence-tolerant midspan section was shape-optimized using the AIRFOILOPT code, which has been in use at RR-NAT (formerly Allison Engine Company) for decades. A generic blade was first optimized at the cruise (design angles). New optimized airfoils shapes were then obtained at discrete inlet flow angle increments between cruise and takeoff (hover), with axial Mach number held constant. After traverse the full range of incidence, the midspan section was re-optimized at the cruise (design) condition. The loss bucket for the midspan section is provided in Figure 7 with the takeoff (hover, $\beta_1 = -2°$) and cruise ($\beta_1 = +40°$) inlet angles noted. A 100 percent N^* operating condition ($\beta_1 = -11°$) corresponding to cruise altitudes is also noted. The coordinates of the final profile (inset in Figure 7) were delivered to NASA for subsequent testing in the transonic linear cascade as described in the following section.

3-D Blading Design/Efficiency-Speed Trend Analysis

Hub, midspan, and tip-sections were radially stacked on their center of gravity and were analyzed using 3-D RANS computations in ADPAC (Ref. 30) as an isolated bladerow. The computations were used to analyze the impact of altitude, turbine pressure ratio, and shaft-speed change. Consistent with the findings illustrated in Figure 6, Rotor 2 efficiency was found to increase by two points in moving from the cruise to takeoff operating condition (Ref. 11).

Experimental Testing of Incidence-Tolerant Blading

The GRC Transonic Turbine Blade Cascade (see Figure 8) has been used to obtain detailed flow and heat transfer data on a wide variety of turbine blade geometries. The tunnel operational capabilities (see Figure 9) enable testing at relevant LPT relative Mach numbers ($0.6 < M_2 < 1$) and inlet turbulence intensities (0.3 percent $< Tu < 15$ percent), over an order-of-magnitude range of Re, and wide range of inlet flow (and incidence) angle settings ($-17° < \beta_1 < +70°$). The cascade has been used previously to acquire heat transfer data sets (Ref. 31). In the present effort, heat transfer rates have proven to be an effective marker for transitional flows of importance to VSPT blading.

E³ Tip-Section Tests

Aerodynamic tests of a 2-D tip section of a NASA/GE Energy Efficient Engine (E³) blade (Ref. 32) were performed as an initial step to get detailed code and model assessment data relevant to a VSPT. Midspan data were obtained 8.6 percent c_x downstream of the blade trailing edge over three blade passages and include total pressure, Mach number, and flow angle. A five-hole pneumatic probe was used, following the methodology described elsewhere (Ref. 33). Sample total pressure data are shown in Figure 10 at $+4.1°$ and $+19.1°$ incidence angles. The incidence angle is defined based on a design-intent $\beta_1 = +29.7°$. The design inlet Reynolds number is $Re_{cx,1} = 6.83 \times 10^5$ and the design pressure ratio is 1.441 giving an isentropic exit Mach number of $M_{2,i} = 0.74$. Other conditions were chosen to obtain as low a Reynolds number as possible within the operating envelope of the facility (Figure 9). The left side of each peak in Figure 10 corresponds to the pressure side of the wake while the right sides correspond to the suction sides. For $i = +4.1°$, the wake widths and depths grow with decreasing Reynolds number but all share the same linear suction surface profile. At a more highly loaded condition of $i = +19°$, the suction sides show significant thickening at lower Reynolds numbers, indicative of rapid boundary layer growth brought about by incipient separation. These effects are anticipated for VSPT blading as well, making this an appropriate test case for predictive model validation.
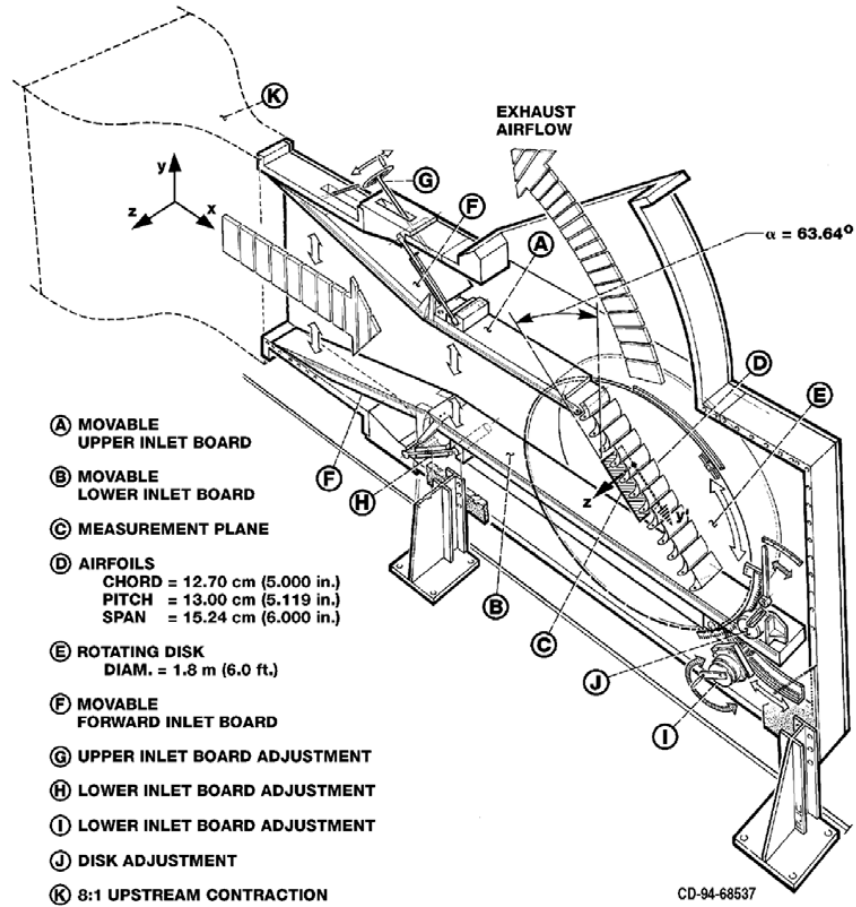
Figure 8.—Schematic drawing of the GRC transonic linear cascade, recently modified for testing incidence-tolerant blading for VSPT.
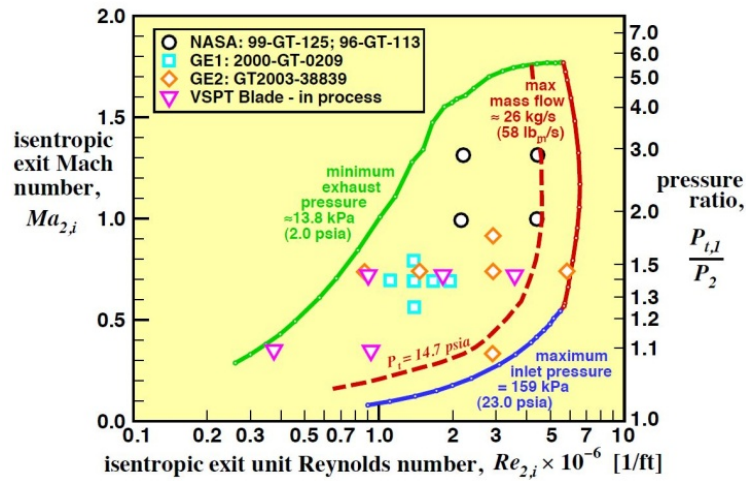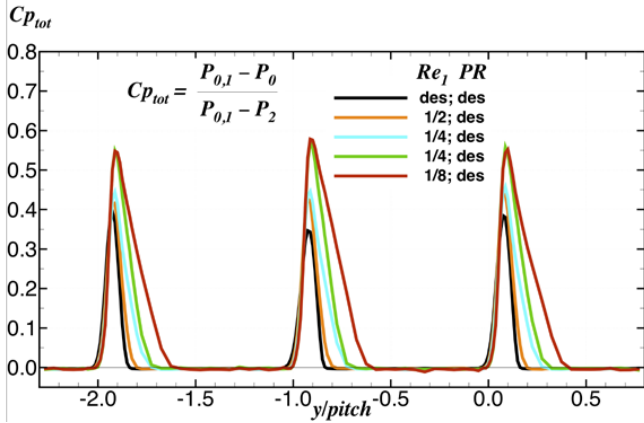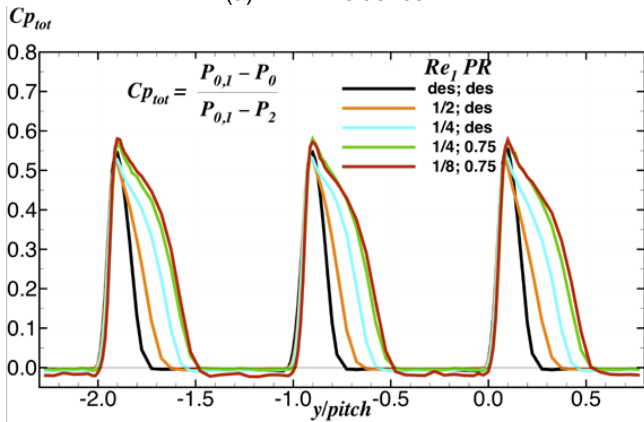

Figure 9.—GRC transonic linear cascade operating map defined by flow boundaries, showing VSPT and previous heat transfer and aerodynamic test points.
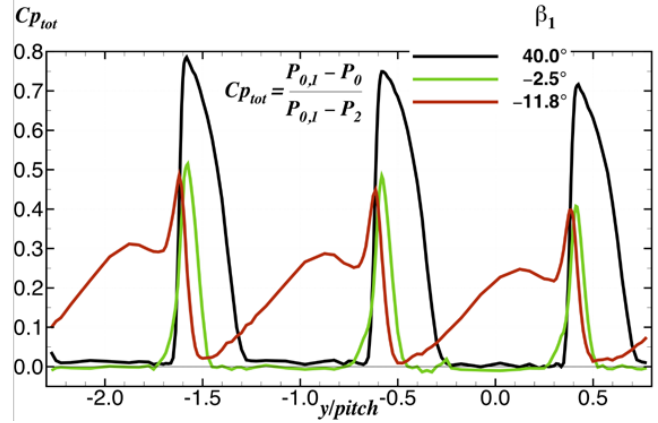
(a) +4.1° incidence

(b) +19.1° incidence

Figure 10.—Aero survey data acquired in the NASA transonic linear cascade at midspan of E^3 blading at design pressure ratio and varying Reynolds number, for two inlet flow angles.
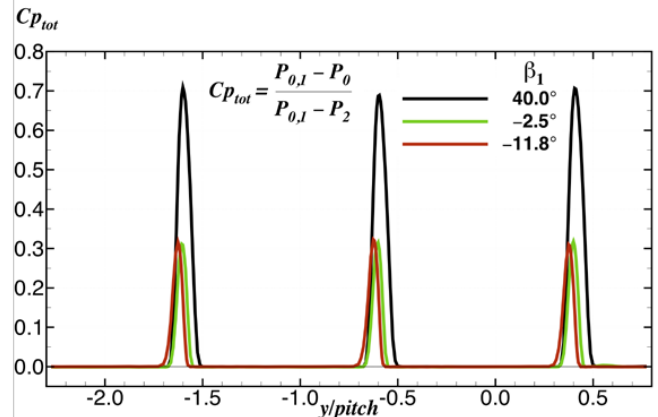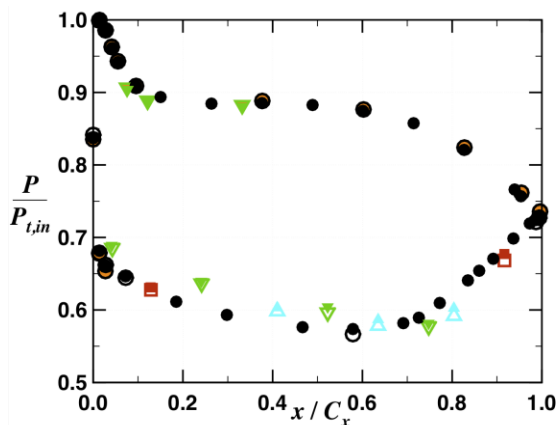

(a) $Re_{cx,2} = 0.212 \times 10^6$, $M_{2,i} = 0.35$

(b) $Re_{cx,2} = 2.120 \times 10^6$, $M_{2,i} = 0.72$

Figure 11.—Aero survey data acquired in the NASA transonic linear cascade at midspan of the RR-NAT designed VSPT blading at various Reynolds numbers, pressure ratios, and inlet flow angles.

Incidence-Tolerant VSPT Blade Tests

During the past year, the cascade facility (NASA CW-22) was modified significantly to extend the range of flow angle setting so as to accommodate high negative incidence testing of relevance to VSPT blading. The tunnel was re-baselined using the E^3 blading by repeating the test points at various inlet flow angles, including the positive incidence angles described in the previous section.

The midspan section of the incidence-tolerant VSPT rotor blading (Figure 7 inset) developed under the RTAPS contract with RR-NAT (Ref. 10) is currently being tested in the modified facility. Loss buckets of the type shown in Figure 7 are being generated for a parametric range of Reynolds numbers. Wake data were acquired 7.0 percent c_x downstream of the VSPT blade trailing edge using a 5-hole probe. A 3-hole boundary-layer probe was used in the region below 4.2 percent of span from the endwall.

Total pressure coefficient data are shown in Figure 11 at the minimum and maximum Reynolds number conditions and over a wide range of inlet (and incidence) angles; $\beta_1 = +40.0°$ ($i = +5.8°$, cruise), $\beta_1 = -2.5°$ ($i = -36.7°$, takeoff), and $\beta_1 = -11.8°$ ($i = -46.0°$, max. incidence). The pressure surface is on the left side of the wakes while the suction surface is on the right. The data clearly show the effects of angle and flow condition on the pressure and suction surface wakes, again making this an appropriate test case for predictive model validation. Midspan data are being acquired at other inlet angles and flow conditions in order to give a more complete assessment of the losses. Full-span data (endwall to midspan) were also acquired at the lowest Reynolds numbers achievable at the design blade pressure ratio ($M_2 = 0.72$) and at incidence-angles corresponding to the cruise ($i = +5.8°$ design-point) and takeoff incidence levels ($i = -36.7°$).

The incidence-tolerant VSPT blades were instrumented with static pressure taps to provide blade loading data to be correlated with the loss measurements. The majority of the pressure taps were located at midspan, but taps were also located at 10, 15, and 30 percent span. The center measurement blade was instrumented most densely, and the suction and pressure surfaces of adjacent blades were instrumented to verify periodicity. Sample blade loading data are shown in Figure 12 for two flow conditions. The loading diagram in Figure 12(b) shows a large cove separation region on the front portion of the pressure surface which leads to the thickening of the pressure surface wake shown in the wake measurements of Figure 11(a) at $\beta_1 = -11.8°$. Conversely, the loading diagram in Figure 12(a) indicates attached flow everywhere, leading to the relatively narrow wakes shown in Figure 11(b). The loading measurements, when analyzed with the wake measurements, provide for a more complete interpretation of the effects of incidence and flow conditions.

(a) $\beta_1 = +40.0°$ ($i = +5.8°$), $Re_{cx,2} = 2.120×10^6$, $M_{2,i} = 0.72$
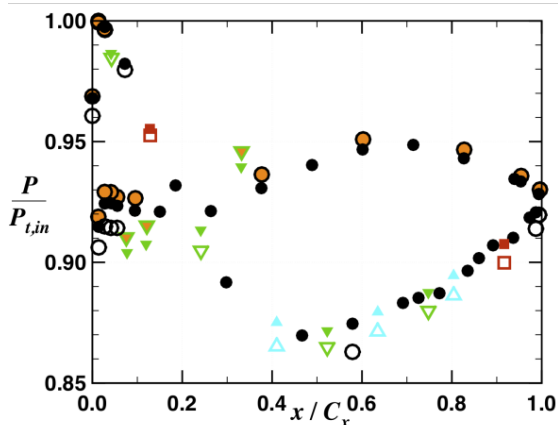
(b) $\beta_1 = -11.8°$ ($i = -46.0°$), $Re_{cx,2} = 0.212×10^6$, $M_{2,i} = 0.35$

Figure 12.—Static pressure blade loading from the incidence-tolerant VSPT blading at various Reynolds numbers, pressure ratios, and inlet flow angles.

Computational Methods

The unit Reynolds numbers of the LCTR VSPT aft-stages are near 50k/in. The low Reynolds number operation admits transitional flow fields with significant laminar regions which are subject to separation induced transition to turbulent flow. The transitional flow is sensitive to the deterministic buffeting of wakes from upstream blade rows (Refs. 5, 26, and 27). Thus, in addition to the difficulty of predicting 3-D transitional flow fields computationally due to turbulence/transition sub-model limitations, the impact of unsteadiness must be included in accurate predictions of turbine performance. The large incidence swings of the VSPT add an additional complication and degree of complexity to the problem as well. An internal effort (Ref. 34) to down-select and validate an accurate turbulence/transition model for RANS computations, and for subsequent implementation in an unsteady RANS (URANS) solver for multistage turbine calculations, is reported in this section.

Turbulence Model for Transitional Flow Fields

Following a year-long investigation of various turbulence modeling approaches suitable for LPT flow fields, the Walters and Leylek (Refs. 35 and 36) model was implemented in the NASA RANS code GlennHT (Ref. 37). The Walters-Leylek (W-L) model is a three-equation (k-ω-k_1), model which accounts for the laminar kinetic energy, k_1, portion of the total intensity of unsteadiness and its natural growth, admitting a mechanism for natural and bypass transition in the RANS sub-model. The model implementation and verification is described in detail elsewhere (Ref. 38). The new code capability was assessed by comparisons of 2-D heat transfer for textbook (Ref. 39) flat plate flow fields and with transition heat transfer data sets obtained from experiments in the NASA transonic linear cascade (Ref. 31). The wall heat transfer data sets were used because heat transfer rates (Nu) provide a strong blade-surface marker for transitional flows. Upon ensuring the satisfactory performance of the transition model for test cases, the flow solver with the improved transition model is used to compute the losses.

Steady-State Heat Transfer Assessments

The results of 2-D and 3-D computations of blade heat transfer and comparison with experimental data for the GE2 blade pack (Ref. 31) are shown in Figure 13 to Figure 15 (reproduced from Ref. 38). The GE2 blade is an extruded 2-D section of a high-turning (127°) power-turbine blade. The data were obtained in the GRC transonic tunnel at two $Re_{cx,2}$ while the pressure ratio (and M_2) was held constant.
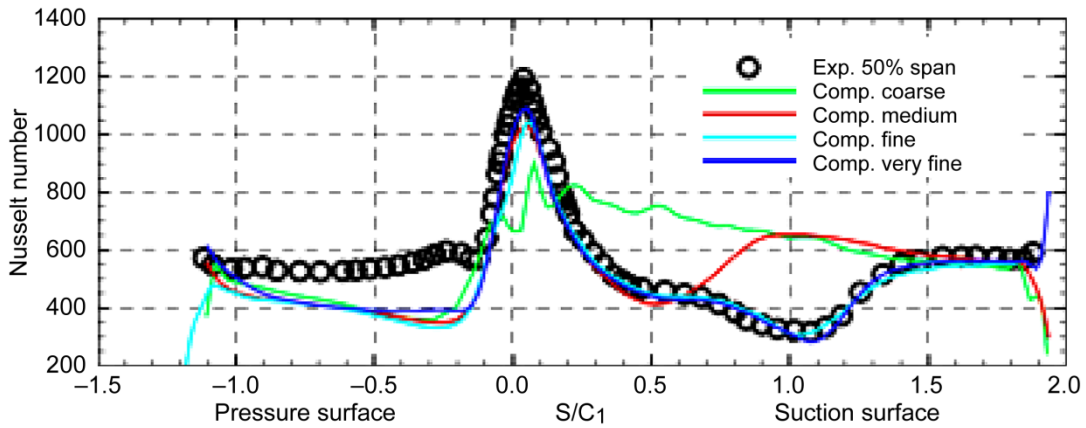
Figure 13.—Two-dimensional computation of Nusselt number against data of Giel et al. (Ref. 31), at $Re_{cx,2} = 375k$.
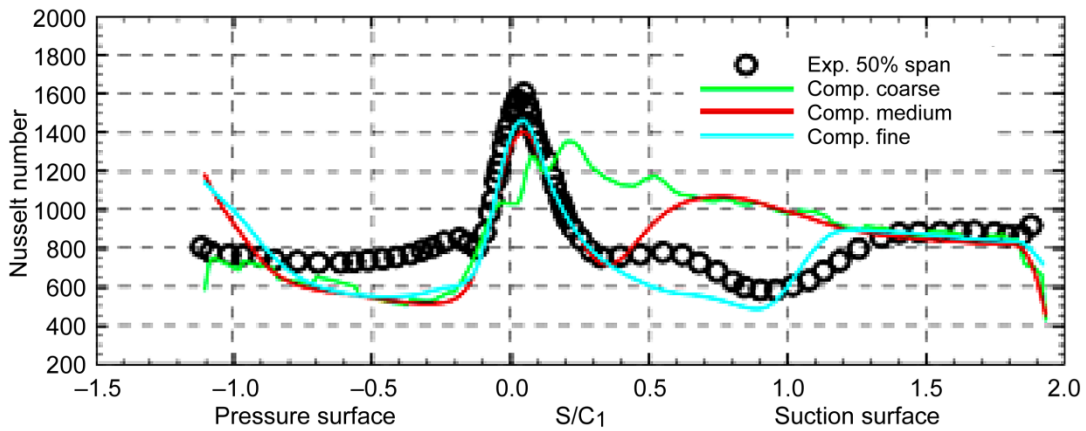

Figure 14.—Two-dimensional computation of Nusselt number against data of Giel et al. (Ref. 31), at $Re_{cx,2} = 621k$.
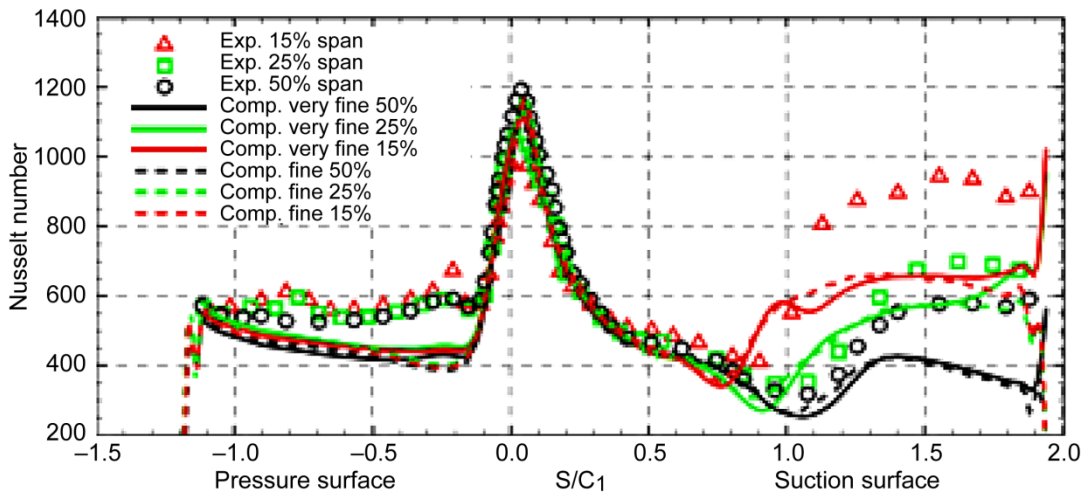

Figure 15.—Three-dimensional computation of Nusselt number and comparison with data from Giel et al. (Ref. 31), $Re_{cx,2} = 375k$.
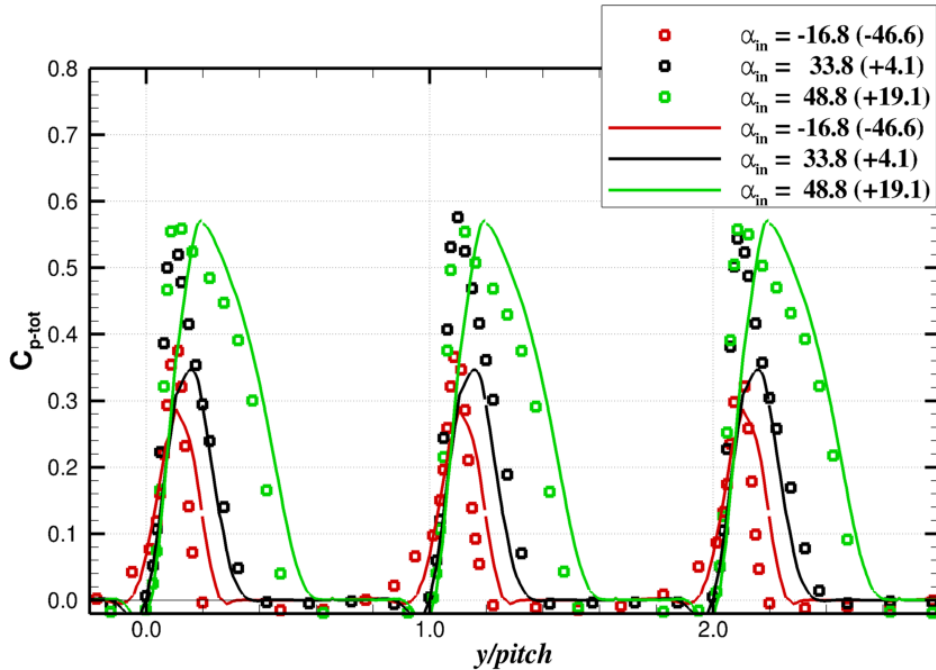
Figure 16.—Comparison of measured[1] (symbols) and computed (curves) total-pressure coefficients at inlet flow angles, α (in deg.), and corresponding incidence angles (parenthesis, in deg.) through VSPT-relevant range of $-47° < i\text{-}i_{des} < +20°$ for E^3 tip-section blading ($Re_{cx,1} = 83k$).

The computed heat transfer rates of the 2-D RANS/W-L computation are in excellent agreement experimental data on the suction side, but heat transfer rates on the pressure-side are under-predicted. The root-cause for the disagreement on the pressure side has not yet been determined. It is noted that the cascade flow field is highly three-dimensional: the inlet boundary layer on each endwall is approximately 15 percent of span and the aspect ratio of the blade pack is less than unity; combined with the high turning of the GE2 cascade, the degree of agreement with 2-D calculations was unexpected.

The 3-D computations for the same cascade are provided in Figure 15. A comparison of the computational and experimental data indicates that the impact of the strong secondary-flow fields and associated high aerodynamic blockage levels may be overestimated by the simulation. The location of transition onset is, nonetheless, well predicted at the three spanwise measurement locations.

Computations of Wake Profiles and Loss in Steady-State Cascade

The agreement for transition between CFD predictions and data from the GE2 cascade test is considered to be quite good. The GlennHT code with the W-L turbulence/transition model was further exercised to compute loss as a function of inci-

dence for a cascade composed of E^3 tip-section blading. Data were again obtained in the GRC transonic linear cascade as described in the previous section. Experimental data from exit surveys with 3-hole p_0 probes were used for verification over a wide (detail) range of incidence angles, exit Mach numbers, and Reynolds numbers. Results for $M_2 = 0.34$ and $Re_{cx,1} = 83k$ are provided here. For the computations, $Tu = 1$ percent and the inlet boundary layer thickness is 49 percent of half-span.

A comparison of computed and measured midspan total-pressure coefficients is provided in Figure 16. The total-pressures are acquired at an axial station 8.6 percent c_x downstream of the trailing edge of the cascade. The incidence angle is defined based on a design-intent $\beta_1 = +29.7°$. Integrated wake deficits (loss) are highest at the positive incidence angles. Interestingly, the agreement between CFD and data is best at extreme positive (most loaded) and negative (unloaded) flow angles; the disagreement in wake depths at the near-design inlet angle ($\beta_1 = +33.8°$, $i\text{-}i_{des} = +4.1$) is substantial and unexplained at this time.

Cross-passage contours of C_{ptot} for incidence angles of approximately $-65°$, $-15°$, $+10°$ and $+30°$ are shown in Figure 17 and iso-surfaces of C_{ptot} are provide in Figure 18. The results in Figure 17 and Figure 18 were carried out at $M_2 = 0.35$ and $Re_{cx,1} = 100$ k. Note that only hub to the midspan symmetry plane is shown. The total-pressure deficits can be identified for each case. The highest loss regions are associated with the vortex cores. This is especially true at the higher positive incidence

---

[1]The data were obtained by A. McVetta and P. Giel, 2011; to be published in AIAA Joint Propulsion Conference, July 2012.
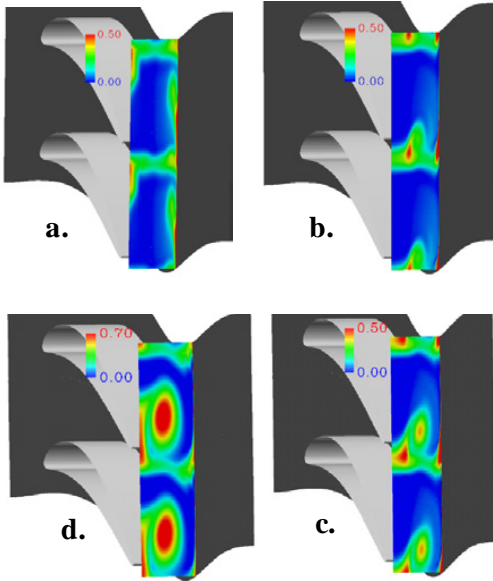
Figure 17.—Total-pressure loss contours (half-span) of E^3 tip-section blading from (clockwise from top-left) for approximate incidences of (a) –65°, (b) –15°, (c) +10°, and (d) +30° (from Ref. 38). Note contour scale change.

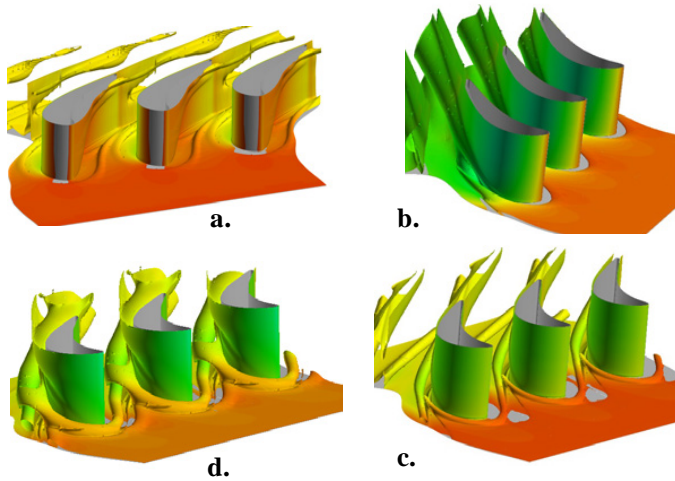Figure 18.—Iso-surfaces of computed loss coefficient of E^3 tip-section blading over half-span for approximate incidence angles of a.) –65°, b.) –25°, c.) +10°, and d.) +30° (from Ref. 38).

angles at which loading and secondary flows are highest. Corresponding flow field structures are provided in Figure 18 in terms of iso-surfaces of total-pressure coefficient. The patterns of C_{ptot} follow, for the most part, the vortical structures highlighted by the iso-surfaces. The contour levels are chosen to illuminate the flow structures, and the iso-surfaces are colored by density to allow better visualization.

For Case (a) with extreme negative incidence, the largest loss near the endwall is due to the interaction of endwall boundary layer and the merged horseshoe/passage vortex system, which stays near the endwall due to the unloading of the blades (Figure 17(a)). The mid-passage increase in loss for Case (a) is due to large flow separation on the pressure side (cove separation) which starts up as a spanwise vortex but turns into a streamwise vortex near midspan. For the other three cases, the midspan loss may be attributed to the suction side leg of horseshoe vortex. High loss is reflected as a bulge in the loss contours in the wake of Case (b). This is highlighted by the better formed local maxima for Cases (c) and (d), and is due to the combined effect of horseshoe and passage vortices. As the loading increases with the incidence, the magnitude and extent of the high loss region increases.

Integrated Results

Using computed wake profiles at spanwise sections between endwall and midspan, loss coefficients based on area-averaged total-pressures were calculated (Figure 19). The resulting loss bucket for the E^3 tip-section blading has extensive (70°) range of incidence at design-point loss levels.

Multistage Turbine Simulations

With intent to improve in-house multistage turbine simulation capability, a NASA supported unsteady turbomachinery code, TURBO (Ref. 40), is currently under further development and evaluation in support of multistage simulation capability for VSPTs with transitional flow. The code improvements were to be implemented in a two-part approach. Firstly, TURBO was to be run against documented multistage turbine geometry so that the mechanics of single-passage per bladerow, phase-lag simulations could be exercised and refined (Ref. 41). Secondly, the W-L turbulence/transition sub-model (Refs. 35 and 36) described above was to be implemented in the TURBO code. The model improvements are described in this section.

Application to Low-Speed Rotating Rig

TURBO (Ref. 40) is a 3-D unsteady RANS (URANS) multi-blade-row, multi-block aero code; the code has been applied to-date primarily to compression systems. As reported earlier (Ref. 41), an assessment of code performance was conducted using the United Technologies Corporation (UTC) large scale rotating rig (LSRR) in 1.5-stage (S1/R1/S2) turbine configuration (Ref. 42). The multistage URANS computations were performed in single-passage per blade-row, phase-lag mode. The simulation details and related analysis are documented elsewhere (Ref. 41). Example time-averaged results are provided in Figure 20, where measured and computed time-averaged loading diagrams on Rotor 1 and Stator 2 of the LSRR are compared and were found to be in acceptable agreement (Ref. 41). Computed results for two flow
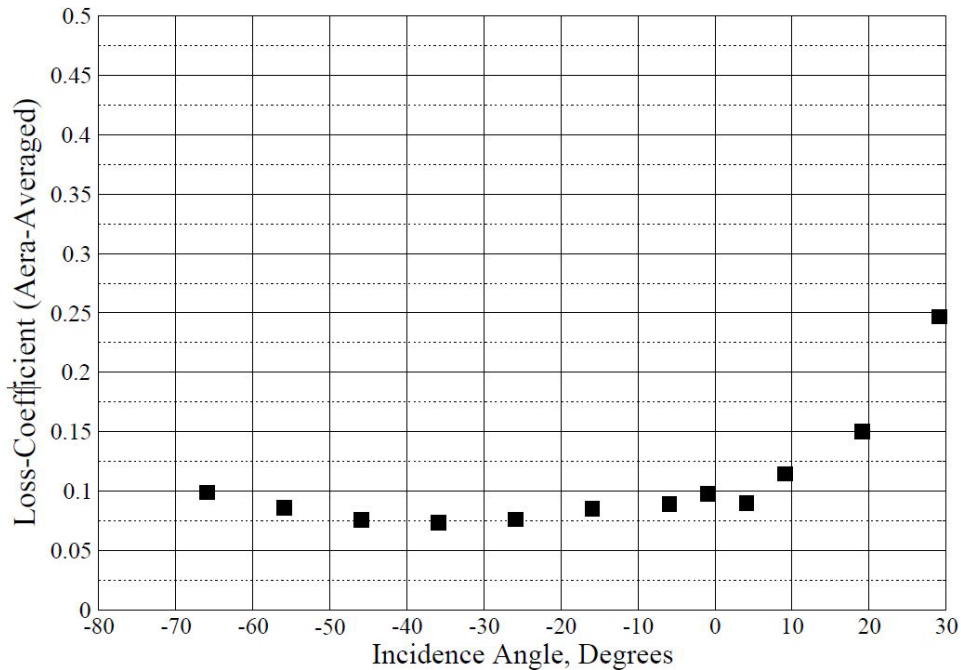
Figure 19.—Loss coefficient based on area-averaged total-pressures of 3-D loss integration of flow fields (Figure 17) as function of incidence angle for extruded E^3 tip-section blading tested in NASA transonic linear cascade at $Re_{cx,2}$ = 100k.
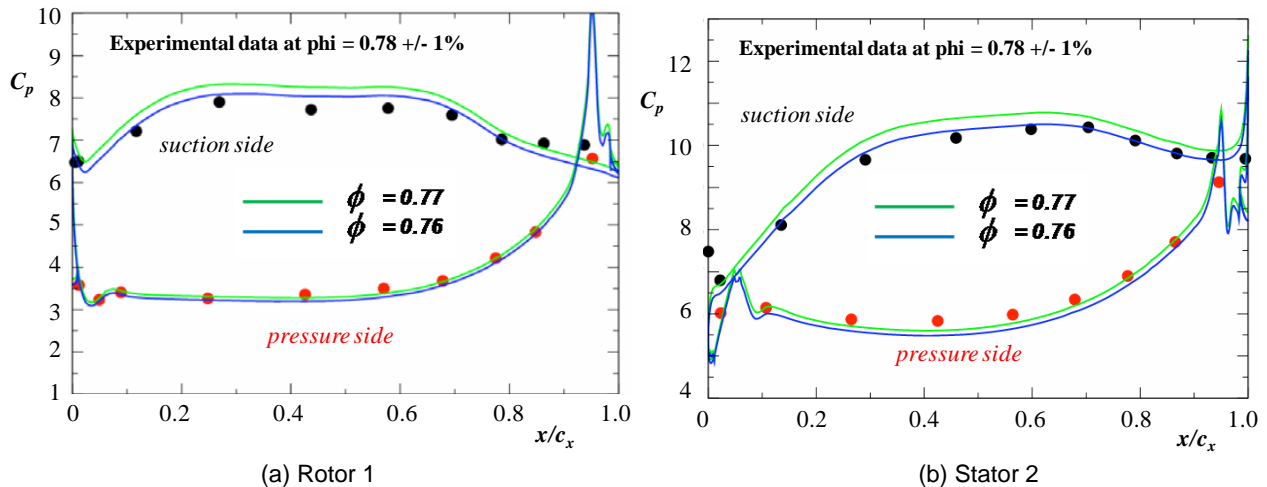

(a) Rotor 1   (b) Stator 2

Figure 20.—Example results from multistage TURBO computation (Ref. 41), showing comparison of computed and measured time-averaged static pressure on (a) Rotor 1 and (b) Stator 2 of Low Speed Rotating Rig (Ref. 42).

coefficients ($\phi = u_x / U$), 0.76 and 0.77, were provided to illustrate the sensitivity of the computed loading diagrams to flow coefficient variation.

The main conclusion from the multistage URANS investigation is that a number of the standard practices used when simulating fans and compressors with TURBO have to be modified for the turbine application. Firstly, clearance gaps will need to be gridded and clearance flows computed; the thickness of the turbine blades renders the tip-clearance

models arbitrary and insufficiently accurate. The validity of wall-functions used with the k-ε model in TURBO is questionable as the mesh is refined to compute the clearance flow. Secondly, because of the large blade turning angles, a mesh topology such as an O-H mixed type or a multi-zone type, as opposed to the H or C type, is more appropriate for turbine simulations. Thirdly, the use of wall functions in the current k-ε turbulence model is not expected to do well in low-Re transitional flow.

Implementation of Walters-Leylek Model in TURBO

The 3-equation W-L turbulence/transitional-flow model (Refs. 35 and 36) described above was implemented in TURBO and is being evaluated currently against heat transfer data from the linear cascade experiments with GE2 blading (Ref. 31) in which the Reynolds numbers are sufficiently low to admit transitional flow. As in the GlennHT implementation described in the previous section, integration to the wall, without the use of wall functions permitted (and warranted) with the W-L model, and therefore the $y^+ \sim 1$ or less at the first point from the wall in future URANS computations.

Rotordynamics

At the initiation of the VSPT research effort, there existed uncertainty about the feasibility of the concept related to the rotordynamic behavior of a multiple-rotor engine operating over a wide speed range (54 to 100 percent of takeoff speed). The source of uncertainty was related to the ability to manage rotor vibration response at operating speeds, and while traversing critical speeds during ramp-up/ramp-down. A rotordynamic feasibility analysis was launched in order to assess the impact of the variable speed concept on an engine in the 7500 shp-class suited for the NASA LCTR. The study (Ref. 6), summarized in this section, was focused on rotor natural frequencies (critical speeds), stability, and steady-state unbalance response of the concept engine with intent to determine the plausibility of the VSPT concept in this size class.

NASA Assessment of Rotordynamics

A rotordynamic model of the notional engine was developed using geometry from a concept engine (Ref. 43) developed for NASA's Large Civil Tilt Rotor (LCTR2) concept vehicle. The front-drive engine model consists of three rotors: a high-speed (33,000 rpm) high-pressure compressor rotor (HP), a moderate-speed (27,500 rpm) low-pressure compressor rotor (LP), and a lower speed (8,100 to 15,000 rpm) VSPT rotor. The size and mass of the various stages, and the overall layout of the engine, were taken from the system study analysis for the engine (Ref. 43).

The rotordynamic model was developed in a commercially available rotordynamics software package that uses a finite element-based, 1-D (axisymmetric), lumped-parameter method to simulate the geometry. A schematic of the three rotor model of the notional engine is provided in Figure 21. A detailed analysis of the feasibility of the concept engine is provided elsewhere (Ref. 6), and a summary of the analyses and findings is given here.

Critical Speed Analysis

An important aspect of any rotating system is the existences of natural frequencies of the rotating structure that can be excited by various sources and potentially lead to failure. Traditionally, aero engines have been designed with relatively fixed-speed power turbine rotors during nominal operation. These rotor systems need to accelerate up to nominal speed, so clearly natural frequencies must be understood; nonetheless, the narrow operational speed range of the typical rotorcraft PT shaft eases the difficulty with which critical speeds can be avoided during steady-state operation. The addition of variable-speed capability in the power turbine complicates the avoidance of natural frequencies in the operating speed range. The larger the operating speed range, the more rotor modes are spanned and may need to be avoided.

For the current VSPT research effort, the rotordynamic model (Figure 21) was exercised to iterate towards a design that eliminated critical speeds from the operating speed range of the PT rotor. In addition, the critical speeds of the LP and HP rotors were calculated to quantify the margin between the critical speed frequencies and the running speed of the respective rotor. No iteration was done on the LP or HP rotors, but the response of the HP and LP rotors could be refined as warranted during detailed design.

A Campbell Diagram for the rotordynamics of the three spools of the notional LCTR engine is provided in Figure 22. The natural frequencies/modes of the three rotors are plotted as a function of rotor speed. The first-engine-order (1EO) line is denoted 1X and represents a synchronous excitation (usually unbalance). The diagram can be used to identify the speeds at which an excitation force—in this case the synchronous unbalance force—coexists with the natural frequencies of the various rotors. The intersections of the 1X line with the natural frequencies define the critical speeds or "crossings." To ensure robust mechanical design, the 1X crossings within the VSPT shaft operating range were avoided; as indicated in Figure 22, there are no 1EO intersections in the power turbine operating range, or near the LP rotor and HP rotor design points.

In order to achieve the desired critical speed behavior, several iterations on the PT rotor design were required. Additional optimization is possible, but may require modifications to the geometry of the LP and HP rotors, and is left to detailed design. In more detailed efforts, higher engine-order crossings may need to be considered as well, as well variations in HP- and LP-shaft speeds over the mission. Nonetheless, feasibility from the standpoint of critical speeds was demonstrated by the preliminary level analysis (Ref. 6).
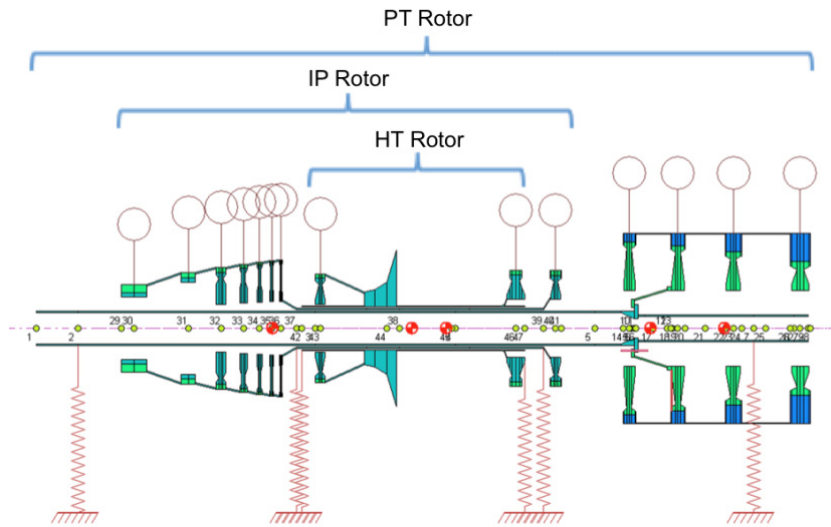
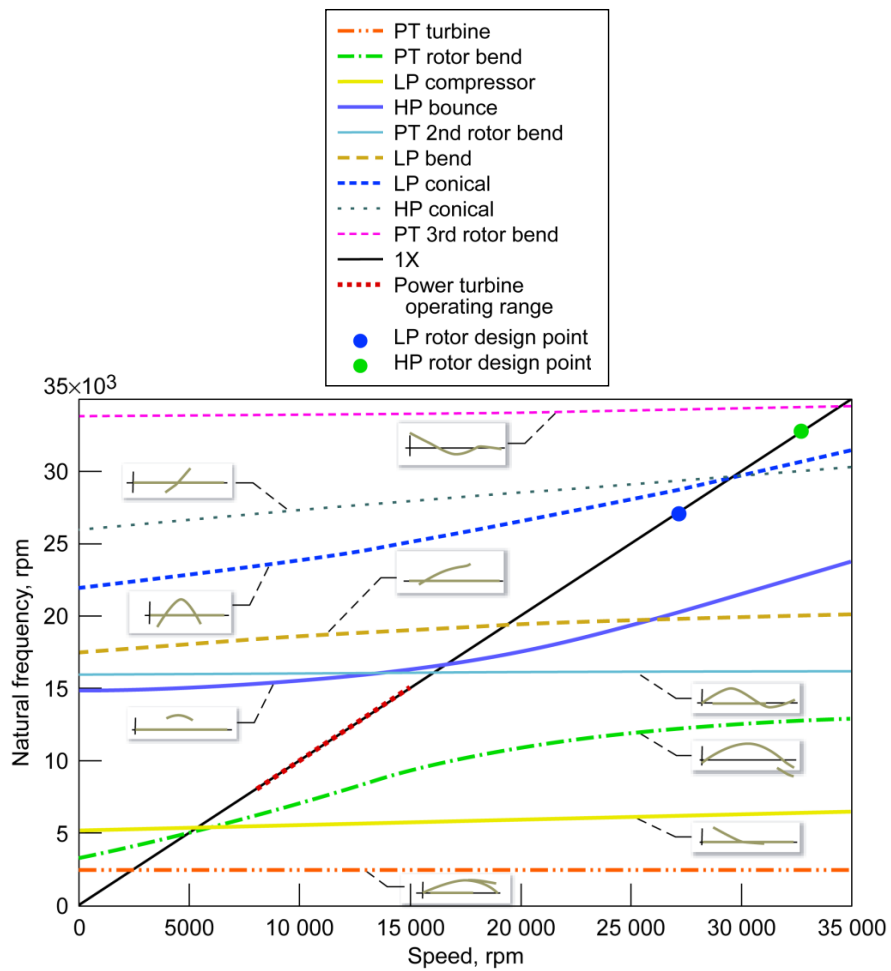Figure 21.—Rotordynamic model of 3-spool, front drive concept engine for NASA LCTR application.

Figure 22.—Campbell Diagram for three rotors of the LCTR concept engine.

Stability Analysis

Stability is an important consideration in aero-engines in which relatively lightweight rotors, spin at relatively high speeds and power, with relatively low damping. This combination of factors can result in an unsafe system susceptible to instability within the operating range. For the conceptual LCTR2 engine, stability could not be analyzed rigorously because the details of the bearings, bearing supports, and housing are unknown; nonetheless, to estimate susceptibility of the design to instability, a simplified stability assessment was undertaken. An artificial amount of damping is added to each bearing support. The amount of damping was incrementally increased at each bearing location until all three rotors of the engine were stable up to their respective maximum operating speeds. In this manner, rather than assessing whether the system was stable with a known amount of damping, the amount of damping needed to achieve stability was determined. Since the required levels of damping were found to be consistent with those of similar applications, stability of the conceptual design was deemed achievable. A detailed description of the stability analysis is provided in Reference 6.

Unbalance Response

Unbalance response sets the rotor balance requirements to ensure that rotor system displacements remain within allowable limits, both at full-speed steady-state operation and during resonance crossings during speed-up and speed-down events. While passing through resonances, the amplitude of motion at the rotor components must not exceed the transient clearances or rubs will occur. Additionally, industry standards for acceptable vibration amplitudes at operating speed must be met, and bearing reaction forces while traversing resonances must be assessed.

To assess the viability of the current conceptual design, a typical new-machine unbalance specification was applied to the rotordynamic model, and the response was calculated over the speed range for each rotor and compared to the accepted industry standard (Ref. 44). The resulting peak-to-peak displacement amplitudes (X_{pk-pk}) calculated for the PT rotor at low and high speeds, and the industry specification are provided in Table II. Since the unbalance response amplitude was found to be less than the standard allowable displacements, this design is considered to be viable from the standpoint of balance considerations. Details of the unbalance response analysis are provided in Reference 6.

TABLE II.—VIBRATION AMPLITUDE FOR
VSPT OF LCTR CONCEPT ENGINE

Speed, rpm	X_{pk-pk} at front bearing location, mm	X_{pk-pk} at rear bearing location, mm	Allowable *pk-pk* amplitude, mm
8100	5.08×10^{-4}	8.89×10^{-3}	2.11×10^{-2}
15000	3.81×10^{-3}	8.64×10^{-3}	1.13×10^{-2}

Industry Assessments of Rotordynamics of LCTR Engines

RR-NAT Assessment

In the NASA RTAPS study contract by RR-NAT (Ref. 11), a growth version of an existing front-drive two-spool AE1107C engine was modified to meet the LCTR requirements. A third stage was added to the VSPT to extend the operational speed-range of the turbine. A revised model of the AE1107C was created for use in the rotordynamics analysis. Subsequently modifications were made to the VSPT concept engine, including PT shaft thickening and modifications to the aft PT bearing placement, and the shaft attachment (from PT disk 1 to 2) in an effort to modify the response and frequency placement of potential responsive modes. The predicted bearing loads for a 1-mm out-of-balance (imbalance response analysis) for the AE1107C baseline and the modified 3-stage VSPT variants, HP and PT rotors, were compared. The bearing loads of the two engine configurations were in close agreement; RR-NAT concluded that the modified AE1107C engine configuration with incorporated VSPT technology is rotordynamically viable (Ref. 11).

Williams International Assessment

An aft-drive engine configuration concept was proposed by WI for the LCTR mission. The VSPT shaft emanates from the aft of the engine, as in the P&WC PT6 turboprop engine, to drive a transmission of fixed reduction gear-ratio. An advantage of this approach is a shorter shaft, relative to shafts of the more common front-drive engine configurations, which could strongly reduce torque and rotordynamics issues. The configuration holds potential engine protection advantages as well. Disadvantages are associated with the need to turn the ambient intake and hot exhaust streams by 180°. The WI analysis was not carried out to a level of detail required to assess the placement of critical modes of the concept engine, however the implication is that the aft-drive configuration offers flexibility in terms of the shaft diameter selection and configuration to achieve required critical speed margins (Ref. 9).

Summary of Rotordynamic Assessments

The conclusion from the NASA in-house and engine company studies is that rotordynamically viable mechanical designs for the VSPT of the LCTR class engine are achievable. The more common front-drive system of the 7500 shp-class engine will likely operate with a supercritical rotor in which VSPT shaft criticals are within the VSPT shaft-speed range. Related rotor-rotor interactions will need to be avoided by mode placement away from steady-state operating points, and responses during transient crossings managed by incorporation of suitable damping levels and shaft thicknesses. The

aft-drive configuration may admit a subcritical VSPT-shaft solution in which all VSPT-shaft modes are above the engine running range.[2] If a subcritical configuration (short, large diameter shaft) were achievable, and the aft-drive configuration proves compatible with aerodynamic, heat load, and packaging constraints, the approach would eliminate VSPT criticals and interactions with other rotor modes within the VSPT running range.

VSPT Component Testing Potential at GRC

The results from an assessment of potential paths to component VSPT component in-house testing at GRC, informed by findings from the VSPT study contracts with RR-NAT (Ref. 11) and WI (Ref. 9), are summarized in this section.

Two in-house approaches to VSPT component testing were considered (Ref. 45): i.) experimental testing would be conducted in an existing power turbine of a T700 engine located in the GRC Engine Components Research Laboratory (ECRL); or, ii.) a new VSPT component rig would be installed in the new single-spool turbine test facility (W-6) at GRC. The objective of the assessment study was to determine the level of compatibility that exists between each research facility and the VSPT component research needs. Preliminary research requirements were defined and the experimental assets available in each facility were examined to determine which approach would provide a greater return on the time and funds to be invested in VSPT experimentation.

Instrumented T700 PT in ECRL

The Engine Component Research Laboratory (ECRL) of GRC is currently configured as a sea-level turboshaft engine test stand. A recently completed assessment has shown that the T700-700 power turbine could be operated with research instrumentation (Figure 23 and Figure 24) in ECRL at the normalized speeds and loads that would simulate the requirements of a notional LCTR mission profile. While provisions for altitude testing exist, the low Reynolds numbers of cruise altitudes could not be matched without a facility upgrade. A rotordynamic model of the T700 power-turbine shaft and support system was used to identify critical speeds of potentially responsive shaft modes. These analyses, along with previously acquired engine vibration data, supported the conclusion that the PT speed could be operated with acceptable shaft response at the design speed and half-speed conditions. The need to modify the engine control system was identified as well.
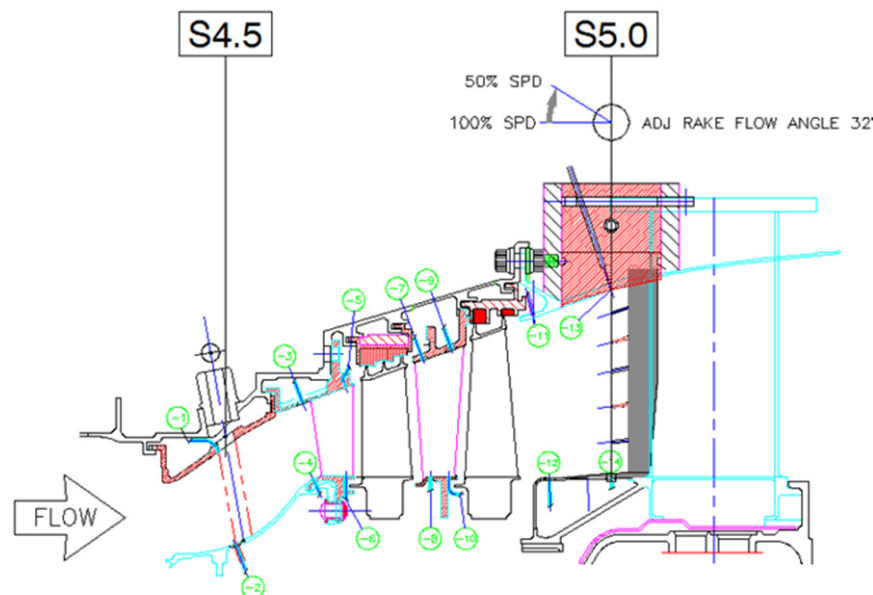

Figure 23.—T700 cross-section, showing proposed positions of rating rakes and static pressure measurements.

---

[2]Note that the analysis and discussion provided in the Williams Int. study contract neither supported nor refuted the supposition that a subcritical VSPT shaft may be enabled by the aft-drive configuration.
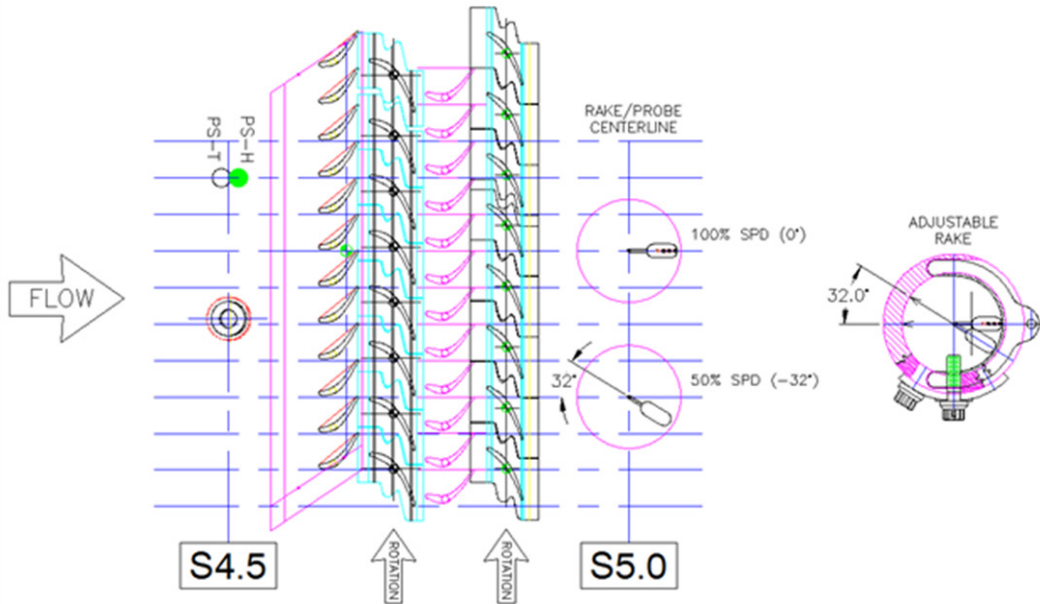
Figure 24.—T700 flat layout showing position of total-temperature and pressure elements and swirl angle capability of downstream rake (Ref. 45).

An instrumentation plan was developed to provide for measurements within the power turbine that would include overall performance measurements (T_0/p_0 rakes at S4.5 and S5.0 of Figure 23) and inter-stage static pressure measurements, as well as provisions for radial surveys of total pressure, total temperature and flow angle (5-hole probe) at the power turbine exit (Station 5.0 of Figure 24). Testing could begin after routine maintenance and safety upgrades to the facility were completed and the aforementioned instrumentation was installed in the T700 power turbine module. These tasks could be performed concurrently and were estimated to take roughly 1.5 years to complete at a relatively low initial cost. As the existing power turbine would be used, this approach would provide data to calibrate analytical and design methods but not to evaluate a specific VSPT design.

VSPT Component Rig in Single-Spool Turbine Facility

The GRC W-6 Single-Spool Turbine Facility (Figure 25) has heated (warm) inlet conditions (940 °F max) and mass-flow-rate (27 lb_m/s max) and pressure (50 psia max.) range suitable for testing components that are full-scale, or are scaled-up, as favorable for detailed measurements of flow profiles and performance. The GRC lab altitude exhaust (2 psia) system would accommodate mission-relevant variations in Reynolds number within current facility capabilities. Heated secondary air supply systems are available as well. Intake flow rates are measured with a calibrated venturi and torque is measured using a stand-alone torque meter. Power transmission and absorption is through a reduction gear-box to

a synchronous generator (Figure 25) with tight speed control vis-à-vis the lab-wide variable frequency system. The W-6 facility will not become available until 2014 due to completion schedule and initial check-out and baseline testing commitments.

As part of the VSPT study contracts, Rolls-Royce NAT and Williams Int. each developed a plan for a cost-effective test approach to conduct component-level research for the LCTR-relevant VSPT. The approach included a research and instrumentation plan, test plan, schedule, and cost estimate. In both studies, the proposed approach was to test a multistage (3.5- or 4-stage) VSPT at scale in the NASA W-6 facility. The experiments would accommodate a multistage VSPT designed to match LCTR engine Mach number, pressure and temperature ratios, and flight Reynolds number requirements. A notional 4-stage test article installation in W-6 and performance rating instrumentation layout from the WI VSPT study contract (Ref. 9) is provided in Figure 26.

Assessment Results

Both the ECRL/T700 engine facility and the W-6 turbine facility were found to be viable options for VSPT experiments. The initial time and funding requirements to prepare an experiment in ECRL were estimated to be less than for the W-6 facility, provided the existing T700 power turbine was retained. Using information documented in the VSPT study contracts(Refs. 9 and 11), the initial cost of the W-6 component approach was estimated to be three to four times higher than the ECRL/T700 approach (using the existing T700 power turbine), and the estimated weekly facility operating costs
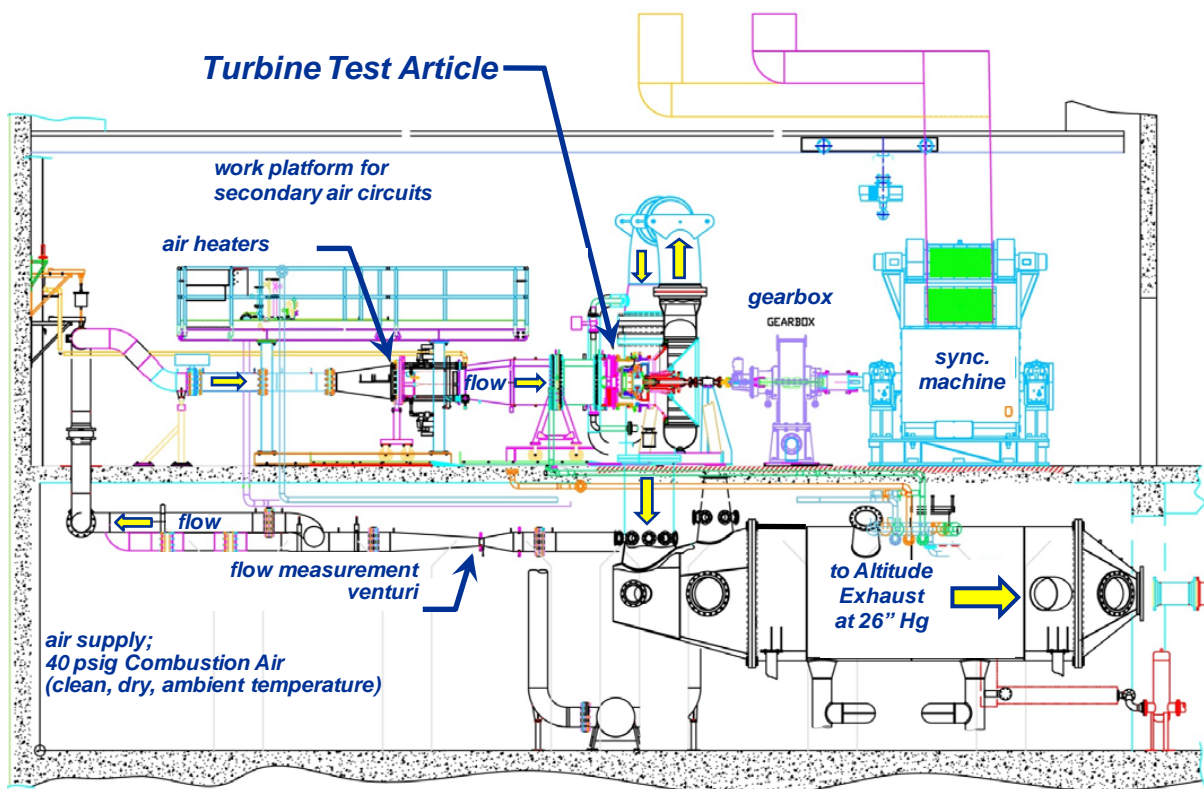
Figure 25.—Schematic diagram of the GRC W-6 Single Spool Turbine Facility.
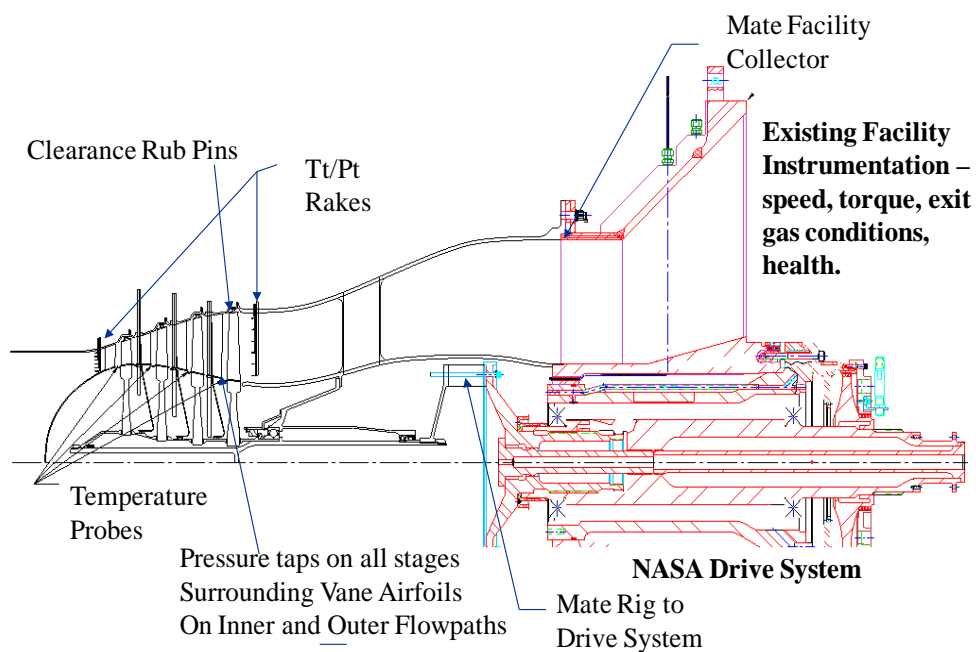

Figure 26.—Williams International 4-stage LCTR VSPT component in GRC W-6 single-spool facility, showing notional rating instrumentation for VSPT turbine-performance mapping (Ref. 9).

were roughly equal. The T700 engine approach would constitute a first step toward verification of the operational capability of the engine and power-absorber over the 50 percent speed range and of the ability to acquire research-quality data from the instrumented power turbine module when integrated in the engine. The PT module would need to be modified/replaced with a compatible VSPT module in a subsequent step. The W-6 facility was found to provide better access for research instrumentation and would permit researchers to evaluate a full-scale power turbine to support the specific aerodynamic research objectives. The W-6 facility is currently the preferred candidate for future VSPT component-level aerodynamic research experiments.

Conclusions

The variable-speed power turbine (VSPT) research effort at GRC was reviewed. In-house and engine-company conceptual design studies have indicated that the VSPT for the NASA LCTR mission will be a 3.5- to 4.5-stage, fixed geometry turbine, dependent in part on the final power requirements and engine power-to-weight-flow levels. Nominal turbine speed operation of 8100 rpm $< N <$ 15000 rpm would correspond to the 54 percent $< N^* <$ 100 percent speed requirement. On- and off-design steady and unsteady 3-D multistage computations completed to-date corroborate meanline analyses in terms of expected increase in turbine efficiency between the cruise (54 percent N^*) to takeoff (100 percent N^*) flight points. The off-design correlations of the meanline tools are critical for such concept studies and improvements at the extreme negative incidence levels are deemed warranted. The VSPT performance maps and insights generated from the VSPT concept design studies and analyses are informing system studies intended to refine the NASA LCTR mission.

Initial experimental results for incidence-tolerant blading tested over a range of VSPT relevant incidence angles were generated in the recently modified NASA transonic linear cascade. The presented results demonstrate that tunnel capability spans the wide range of Reynolds numbers needed to test blading from fully turbulent to transitional flow conditions.

Implementation of the Walters-Leylek turbulence model into in-house 3-D RANS and URANS solvers was described. The W-L model is found to predict accurately the critical suction-side transition, based on comparisons with steady-state heat transfer data previously obtained in the transonic linear cascade. Validation using unsteady data from a high-speed multistage component rig remains for future work.

Conceptual design level rotordynamics analyses, conducted in-house and through the VSPT study contracts with industry, indicate that rotor-dynamically viable engine concepts are obtainable for the 7500 shp-class engine with VSPT.

Finally, two paths to engine testing using internal assets were explored and found to be viable. The preferred path to component test is the use of a turbine test facility with mission Reynolds number test capability, such as the NASA W-6 Single-Spool Turbine Facility.

References

1. Johnson, W., Yamauchi, G. K., and Watts, M. E., "NASA Heavy Lift Rotorcraft Systems Investigation," NASA/TP—2005-213467, Sep. 2005.
2. Acree, C. W., Hyeonsoo, Y., and Sinsay, J. D., "Performance Optimization of the NASA Large Civil Tiltrotor," *Proc. Int. Powered Lift Conf.*, Jul. 2008.
3. Wilkerson, J. B. and Smith, R. L., "Aircraft System Analysis of Technology Benefits to Civil Transport Rotorcraft," NASA/CR–2009-214594, Jun. 2009.
4. Welch, G. E., "Assessment of Aerodynamic Challenges of a Variable-Speed Power Turbine for Large Civil Tilt-Rotor Application," *Proc. AHS Int. 66th Ann. Forum*, May, 2010; also NASA/TM—2010-216758, Aug. 2010.
5. Hourmouziadis, J., "Aerodynamic Design of Low Pressure Turbines," in *Blading Design for Axial Turbomachines*, AGARD-LS-167, 1989, pp. 8-1 to 8-40.
6. Howard, S. A., "Rotordynamic Feasibility of a Conceptual Variable-Speed Power Turbine Propulsion System for Large Civil Tilt-Rotor Applications," *Proc. AHS Int. 68th Ann. Forum*, TX, May 2012; also NASA/TM—2012-217134, May 2012.
7. Stevens, M. A., Handschuh, R. F., Lewicki, D. G., "Variable/Multispeed Rotorcraft Drive System Concepts," NASA/TM—2009-215456; also ARL-TR-4728, Mar. 2009.
8. Litt, J. S., Edwards, J. M., DeCastro, J. A., "A Sequential Shifting Algorithm for Variable Rotor Speed Control," NASA/TM—2007-214842, June, 2007; also, ARL–TR–4086, June 2007.
9. Suchezky, M., "Variable-speed power turbine for the Large Civil Tilt Rotor," NASA/CR—2012-217424, Feb. 2012.
10. Ford, A., Turner, E., Bloxham, M., Gegg, S., King, B., Harris, C., Bell, M., Eames, D., "Variable-Speed Power-Turbine Component Research Plan," NASA/CR—2012-217423, Feb. 2012.
11. Ford, A., Bloxham, M., Turner, E., Clemens, E., Gegg, S., "Design Optimization of Incidence-Tolerant Blading Relevant to Large Civil Tilt-Rotor Power Turbine Applications," NASA/CR—2011-217016, 2012.
12. Snyder, C. A. and Thurman, D. R., "Gas Turbine Characteristics for a Large Civil Tilt-Rotor (LCTR)," *Proc. AHS Int. 65th Ann. Forum*, May 2009; also NASA/TM—2010-216089, Feb, 2010.
13. Welch, G. E., "Computational Assessment of the Aerodynamic Performance of a Variable-Speed Power Turbine for Large Civil Tilt-Rotor Application," *Proc. AHS Forum 67*, May 2011; also NASA/TM—2011-217124, Nov. 2011.
14. Clark, J. P., Koch, P. J., Ooten, M. K., Johnson, J. J., Dagg, J., McQuilling, M. W., Huber, F, and Johnson, P.

D., "Design of Turbine Components to Answer Research Questions in Unsteady Aerodynamics and Heat Transfer," AFRL-RZ-WP-TR-2009-2180, Sep. 2009.

15. Gier, J., Franke, M., Hübner, N. and Shröder, T., "Designing LP Turbines for Optimized Airfoil Lift," *J. Turbomachinery*, **132**, Jul. 2010, pp. 031008-1 to -12.

16. D'Angelo, M., "Wide Speed Range Turboshaft Study," NASA/CR—1995-198380, Aug. 1995.

17. Smith, S. F., "A Simple Correlation of Turbine Efficiency," *J. Royal Aero. Soc.*, **69**, 1965, pp. 467-470.

18. Oates, G. C, *Aerothermodynamics of Aircraft Engine Components,* AIAA Education Series, 1985.

19. Ainley, D. G. and Mathieson, G. C. R., "A Method of Performance Estimation for Axial-Flow Turbines," Aeronautical Research Council (ARC), R&M 2974, 1957.

20. Dunham, J. and Came, P. M., "Improvements to the Ainley-Mathieson Method of Turbine Performance Prediction," *J. Eng. for Power*, Jul. 1970, pp. 252-256.

21. Kacker S. C., and Okapuu. U., "A Mean Line Prediction Method for Axial Flow Turbine Efficiency," *J. Eng. Power*, **104**, Jan. 1982, pp. 111-119.

22. Chima, R. V., "Calculation of Multistage Turbomachinery Using Steady Characteristic Boundary Conditions," AIAA-98-0968, Jan. 1998; also NASA/TM—1998–206613, Jan. 1998.

23. Welch, G. E., "Computational Study of the Impact of Unsteadiness on the Aerodynamic Performance of a Variable-Speed Power Turbine," AIAA-2012-937, Jan. 2012; also NASA/TM—2012-217425, 2012.

24. Rose, M., Schüpbach, P., Mansour, M., "The Thermodynamics of Wake Blade Interaction in Axial Flow Turbines: Combined Experimental and Computational Study," ASME GT2009-59655, Jun. 2009.

25. Adamczyk, J. J., "Model Equation for Simulating Flows in Multistage Turbomachinery," ASME GT1985-226, 1985.

26. Haselbach, F., Schiffer, H.-P., Horsman, M., Dressen, S., Harvey, N., and Read, S., "The Application of Ultra High Lift Blading in the BR715 LP Turbine," *J. Turbomachinery*, **124**, Jan. 2002, pp. 45-51.

27. Halstead, D. E., Wisler, D. C., Okishii, T. H., Walker, G. J., Hodson, H. P, Shin, H-W., "Boundary Layer Development in Axial Compressors and Turbines: Part 3 of 4—LP Turbines," *J. Turbomachinery*, **119**, 1997, p. 225.

28. Ni, R-H, Humber, W., Fan, G., Johnson, P. D, Downs, J., Clark, J. P., Koch, P. J., "Conjugate Heat Transfer Analysis of a Film-Cooled Turbine Vane," ASME GT2011-45920, Jun. 2011.

29. Robuck, M., Wilkerson, J., Zhang, Y., Snyder, C., Nordstrom, C., "Design Study of Propulsion and Drive Systems for the Large Civil Tiltrotor (LCTR2) Rotorcraft," *Proc. AHS 67th Ann. Forum*, May 2011.

30. Hall, E. J., and Delaney, R. A., "Investigation of Advanced Counter-rotation Blade Configuration Concepts for High Speed Turboprop Systems: Task V - ADPAC User's Manual," NASA/CR—1995-195472, 1995.

31. Giel, P. W., Boyle, R. J., and Bunker, R. S., "Measurements and Predictions of Heat Transfer on Rotor Blades in a Transonic Turbine Cascade," *J. Turbomachinery*, **126**, Jan. 2004, pp. 110-121.

32. Timko, L. P., "Energy Efficient Engine High Pressure Turbine Component Test Performance Report," NASA/CR—1984-168289, 1984.

33. Giel, P. W., Thurman, D. R., Lopez, I., Boyle, R. J., VanFossen, G. J., Jett, T. A., Camperchioli, W. P., La, H., "Three-Dimensional Flow Field Measurements in a Transonic Turbine Cascade," ASME 96-GT-113, Jun, 1996; also NASA/TM—1996-107388 and ARL-TR-1252.

34. Ameri, A. A., "Implementation of a Transition Model in a NASA Code and Validation using Heat Transfer Data on a Turbine Blade," NASA/CR—2012-217436, 2012.

35. Walters, D. K., Leylek, J. H., "A New Model for Boundary Layer Transition Using a Single-Point RANS Approach," *ASME Journal of Turbomachinery*, **126**, (1), 2004, p. 193.

36. Walters, D. K., Leylek, J. H., "Computational Fluid Dynamics Study of Wake-Induced Transition on a Compressor-Like Flat Plate," *ASME Journal of Turbomachinery*, **127**, (1), 2005, p. 52.

37. Steinthorsson, E., Liou, M.S., and Povinelli, L.A., "Development of an Explicit Multiblock/Multigrid Flow Solver for Viscous Flows in Complex Geometries," AIAA-93- 2380, 1993.

38. Ameri, A. A., "Use of Transition Modeling to Enable the Computation of Losses for Variable-Speed Power Turbine," ASME GT2012-69591, Jul. 2012; also NASA/CR—2012-217435, 2012.

39. Incropera, F. P. and DeWitt, D. P., *Fundamentals of Heat Transfer*, Wiley, NY, 1981.

40. Chen, J. P. and Briley, W. R., "A Parallel Flow Solver for Unsteady Multiple Blade Row Turbomachinery Simulations," ASME GT2001-0348, Jun, 2001.

41. To, W. M., "Unsteady Aero Computation of a 1-1/2 Stage Large Scale Rotating Turbine", NASA/CR—2012-217438, 2012.

42. Dring, R.P., Fair, M.F., Joslyn, H.D., Power, G.D., and Verdon, J.M., "The Effect of Inlet Turbulence and Rotor/Stator Interactions on the Aerodynamics and Heat Transfer of a Large Scale Rotating Rig Turbine Model, Vol. I – Final Report," NASA/CR—1987-4079, 1987.

43. Snyder, C.A., and Thurman, D.R.: "Effects of Gas Turbine Component Performance on Engine and Rotary Wing Vehicle Size and Performance," NASA/TM—2010-216907, Nov. 2010.

44. International Standard ISO 1940-1:2003/Cor. 1:2005(E), International Organization for Standardization, Switzerland, 2005, p. 11.

45. Skoch, G. J., Griffin, T. A., Stevens, M. A., Howard, S. A., Welch, G. E., and Giel, P. W., "Assessment of Variable-Speed Power-Turbine Component Test Capability at NASA Glenn Research Center," NASA/TM—2012-217422, 2012.

REPORT DOCUMENTATION PAGE

1. REPORT DATE *(DD-MM-YYYY)* 01-07-2012	2. REPORT TYPE Technical Memorandum	3. DATES COVERED *(From - To)*

4. TITLE AND SUBTITLE
Variable-Speed Power-Turbine Research at Glenn Research Center

5a. CONTRACT NUMBER

5b. GRANT NUMBER

5c. PROGRAM ELEMENT NUMBER

6. AUTHOR(S)
Welch, Gerard, E.; McVetta, Ashlie, B; Stevens, Mark, A.; Howard, Samuel, A.; Giel, Paul, W.; Ameri, Ali, A.; To, Waiming; Skoch, Gary, J.; Thurman, Douglas, R.

5d. PROJECT NUMBER

5e. TASK NUMBER

5f. WORK UNIT NUMBER
WBS 877868.02.07.03.01.02.02

7. PERFORMING ORGANIZATION NAME(S) AND ADDRESS(ES)
National Aeronautics and Space Administration
John H. Glenn Research Center at Lewis Field
Cleveland, Ohio 44135-3191

8. PERFORMING ORGANIZATION REPORT NUMBER
E-18186

9. SPONSORING/MONITORING AGENCY NAME(S) AND ADDRESS(ES)
National Aeronautics and Space Administration
Washington, DC 20546-0001

10. SPONSORING/MONITOR'S ACRONYM(S)
NASA

11. SPONSORING/MONITORING REPORT NUMBER
NASA/TM-2012-217605

12. DISTRIBUTION/AVAILABILITY STATEMENT
Unclassified-Unlimited
Subject Categories: 02, 01, 03, 07, 34, and 09
Available electronically at http://www.sti.nasa.gov
This publication is available from the NASA Center for AeroSpace Information, 443-757-5802

13. SUPPLEMENTARY NOTES

14. ABSTRACT
The main rotors of the NASA Large Civil Tilt-Rotor (LCTR) notional vehicle operate over a wide speed-range, from 100 percent at takeoff to 54 percent at cruise. The variable-speed power turbine (VSPT) offers one approach by which to effect this speed variation. VSPT aerodynamics challenges include high work factors at cruise, wide (40° to 60°) incidence-angle variations in blade and vane rows over the speed range, and operation at low Reynolds numbers. Rotordynamics challenges include potential responsiveness to shaft modes within the 50 percent VSPT speed-range. A research effort underway at NASA Glenn Research Center, intended to address these key aerodynamic and rotordynamic challenges, is described. Conceptual design and 3-D multistage RANS and URANS analyses, conducted internally and under contract, provide expected VSPT sizing, stage-count, performance and operability information, and maps for system studies. Initial steps toward experimental testing of incidence-tolerant blading in a transonic linear cascade are described, and progress toward development/improvement of a simulation capability for multistage turbines with low Reynolds number transitional flow is summarized. Preliminary rotordynamics analyses indicate that viable concept engines with 50 percent VSPT shaft-speed range. Assessments of potential paths toward VSPT component-level testing are summarized.

15. SUBJECT TERMS
Turbine aerodynamics; Rotordynamics; Turbine cascade; CFD; Gas turbine engine

16. SECURITY CLASSIFICATION OF:			17. LIMITATION OF ABSTRACT	18. NUMBER OF PAGES	19a. NAME OF RESPONSIBLE PERSON STI Help Desk (email:help@sti.nasa.gov)
a. REPORT U	**b. ABSTRACT** U	**c. THIS PAGE** U	UU	30	**19b. TELEPHONE NUMBER** *(include area code)* 443-757-5802